

ESSENTIAL CONSIDERATIONS FOR THE IMPLEMENTATION OF MEMBRANE DISTILLATION CRYSTALLISATION IN THE TREATMENT OF HYPERSALINE BRINES

Report to the

Water Research Commission

by

Jeeten Nathoo¹, Abdul Azeez Ismail², Mujahid Aziz² & Dyllon Randall³

¹Saintelligent Dynamics

²Cape Peninsula University of Technology

³University of Cape Town

WRC Report No. 2763/1/22

ISBN 978-0-6392-0469-7

July 2022

Obtainable from

Water Research Commission

Private Bag X03

Gezina

PRETORIA, 0031

orders@wrc.org.za or download from www.wrc.org.za

DISCLAIMER

This report has been reviewed by the Water Research Commission (WRC) and approved for publication. Approval does not signify that the contents necessarily reflect the views and policies of the WRC, nor does mention of trade names or commercial products constitute endorsement or recommendation for use.

Executive Summary

The generation of brine waste streams emanating from water treatment processes such as reverse osmosis (RO), multi-stage flash (MSF) and multi-effect distillation (MED) are a major concern for the environment. A 2019 global outlook study revealed that there are 15906 operational desalination plants globally, producing around 142 million m³/day of brine. Reverse osmosis (69%), multi-stage flash (18%) and multi-effect distillation (7%) account for 94% of the total hypersaline brine volumes generated globally. The aqueous characteristics of these hypersaline brines are generally classified into two main categories: (i) monovalent ion dominant, non-scaling brines, e.g. sodium chloride dominant brines emanating from seawater desalination processes, and (ii) divalent and trivalent ion dominant brines with scaling and/or fouling potential, e.g. brines emanating from the desalination of brackish water.

Brine waste-handling and disposal methodologies are largely contingent on the geography in the vicinity of the plant generating the brine and include discharge into oceans, inland water bodies such as rivers, surface dams and sewers, as well as deep-well injection and brine storage in waste evaporation ponds. These methodologies are not environmentally sustainable and consequently, brine treatment towards achieving minimal liquid discharge (MLD) or ultimately zero liquid discharge (ZLD) in a cost-effective way has become a major challenge. In most cases, although the first 90-95% of the waste stream can be treated relatively cost-effectively using well-established, conventional, commercially available technologies, the capital equipment costs and operating costs associated with treating the remaining 5% using conventional thermal evaporation process typically tends to double the overall treatment cost.

Emerging technologies under investigation for the treatment of brines include forward osmosis (FO), eutectic freeze crystallisation (EFC), osmotically assisted reverse osmosis (OARO) and membrane distillation crystallisation (MDC).

Membrane Distillation Crystallisation (MDC) offers a sustainable wastewater treatment option for saline and hypersaline effluent streams. This is particularly so when utilising excess waste heat from peripheral processes to produce pure water. In addition to this, the generation of potentially usable salts converts a waste effluent stream into one with saleable products of value that can either be reused, recycled, or sold to offset water treatment costs towards driving down the unit cost per m³ of treated water.

The objectives of this study were to identify quintessential considerations, mainly related to key membrane characteristics and performance criteria, when assessing the viability of implementing and selecting MDC over alternative technologies. Specifically, the study focussed on:

- i) Determining the minimum acceptable flux below which membrane distillation as an emerging technology becomes commercially unviable relative to existing commercial brine treatment technologies
- ii) Development of a flux prediction model that uses brine salinity, feed temperature and membrane pore size as input variables to yield the predicted flux as the response variable. The utility in this model lies in its ability to quickly ascertain whether any specific brine under consideration meets the minimum acceptable flux criterion described in (i) above

- iii) Development of a decision-making tool for industrial practitioners to ascertain whether membrane distillation is a suitable alternative for the treatment of hypersaline brines and furthermore to provide operating parameter guidelines for a specific brine being investigated based on its aqueous and scaling characteristics.

A Direct Contact Membrane Distillation (DCMD) system was used to conduct the experimental work related to this study.

Of the various membrane characteristics investigated, membrane pore size was identified as the key variable in terms of membrane selection. As a result, the study focussed exclusively on two polyvinylidene fluoride (PVDF) membranes, which were characteristically similar in all respects other than their pore sizes with one having a pore size of 0.22 μm and the other 0.45 μm .

Two types of hypersaline brines were investigated: (i) Type 1 Brine – a monovalent ion dominant, non-scaling/fouling brine and (ii) Type 2 Brine – a divalent and trivalent ion dominant brine with significant scaling and/or fouling potential. The differences in Type 1 and Type 2 brines provided an adequate range in variability with respect to the aqueous characteristics of the diverse range of brines emanating from the industrial and mining sectors.

Commercial viability is strongly influenced by the achievable flux, which in turn determines the total membrane surface area required and provides an indication of the overall system costs. The minimum acceptable flux below which MDC as an emerging technology becomes commercially unviable relative to the existing commercial brine treatment technologies of multi-effect distillation (MED) and mechanical vapour recompression evaporation (MVC) was determined to be 18 L/m²·hr.

The flux prediction model developed for Type 1 brine (NaCl.H₂O solution) was based on an experimental matrix with the input variables being feed concentration (35, 50 and 65 g/l), feed temperature (40°C, 60°C and 80°C) and membrane pore size (0.22 μm and 0.45 μm). The significance tests for the regression models and individual model coefficients were determined for all responses using statistical methods. The flux prediction models for 0.22 μm and 0.45 μm membrane pore sizes, whose quadratic models showed a very a good data fit are shown below (T represents the feed temperature [°C], and C represents the feed concentration [g/L]):

$$flux_{GVHP,0.22} = 27.81439 - 0.748949T - 0.561393C - 0.000682TC + 0.015660T^2 + 0.005191C^2$$

$$flux_{HVHP,0.45} = 19.25581 - 0.643455T - 0.499364C - 0.000682TC + 0.015660T^2 + 0.005191C^2$$

Additional key findings from the experimental investigation into the effects of membrane pore size, transmembrane temperature differential and feed water characteristics on the resultant flux rate and scaling/fouling characteristics for prepared **Type 1 brine** were as follows:

- i) Temperature had the greatest influence on increasing the permeate flux and that the higher the feed temperature, the higher the flux. At a feed temperature of 40°C, the fluxes were below the minimum 18 L/m²-hr for both membrane pore sizes suggesting that the feed temperatures between 60-80°C would be ideal
- ii) The maximum fluxes obtained for the 0.22 µm and 0.45 µm pore size membranes at 80°C were 54.2 L/m²-hr and 54.7 L/m²-hr respectively. These fluxes were well above the minimum acceptable flux of 18 L/m²-hr for MDC demonstrating potential commercial viability
- iii) Changes in feed concentration for the monovalent solutions did not have any significant effect on MD performance, which was largely attributed to the non-scaling/fouling characteristics of the brine. This is a major benefit for MDC to be used to treat hypersaline brines at elevated concentrations significantly beyond those capable of being treated by other emerging or commercially available technologies
- iv) At elevated feed total dissolved concentrations (TDS) in excess of 200 g/L, i.e. representing conditions at the tail end of the MDC process, the 0.22 µm pore size PVDF membranes were better suited in terms of achieving a 22.5% higher flux rate (25.54 L/m²-hr) and better salt rejection at higher overall recoveries for Type 1 brines when compared to 0.45 µm pore size membranes.

Similarly, key findings from the experimental investigation into the effects of membrane pore size, transmembrane temperature differential and feed water characteristics on the resultant flux rate and scaling/fouling characteristics for prepared **Type 2 brine** were as follows:

- i) Similar to Type 1 brine, temperature had the greatest influence on increasing the permeate flux and that the higher the feed temperature, the higher the flux
- ii) The maximum fluxes obtained for the 0.22 µm pore size membrane at feed TDS concentrations of 11870 mg/L and 27025 mg/L and 80°C were 48.03 L/m²-hr and 28.67 L/m²-hr respectively. The maximum fluxes obtained for the 0.45 µm pore size membrane at feed TDS concentrations of 11870 mg/L and 27025 mg/L and 80°C were 40.13 L/m²-hr and 26.17 L/m²-hr respectively. Although, the fluxes for Type 2 brines were lower than those for Type 1 brines owing to the scaling nature of the Type 2 brine and the resultant increase in suspended solids, these fluxes were still above the minimum acceptable flux of 18 L/m²-hr for the commercial viability of MDC
- iii) The 0.45 µm pore size membrane performed significantly better than the 0.22 µm pore size membrane at elevated suspended solids concentrations in terms of permeate flux and salt rejection. However, beyond a suspended solids concentration of 3000 mg/L for the 0.22 µm pore size membranes and 3200 mg/L for the 0.45 µm pore size there was a sharp decline in MD performance both in terms of permeate flux and salt rejection
- iv) At elevated feed total dissolved concentrations (TDS) and suspended solids concentrations up to 3200 mg/L, 0.45 µm pore size PVDF membranes were better suited in terms of achieving higher flux rates at higher overall recoveries for Type 2 brines
- v) Despite the elevated total suspended solids concentrations, the flux achieved using the 0.45 µm pore size membrane was significantly higher than that for the 0.22 µm pore size membrane

vi) Furthermore, the flux achieved using the 0.45 µm pore size membrane was greater at lower impeller stirrer speeds suggesting that larger particle sizes which are less likely to enter the membrane pores and cause wetting, promote higher flux rates and should be prioritised in terms of the reactor control.

Using the information obtained from the experimental investigations, a decision-making tool was developed to assist prospective users of membrane distillation technology in assessing the viability of using membrane distillation for brine treatment. Furthermore, the decision-making tool provided guidelines in terms of membrane selection and process operating conditions for specific types of brines.

This study aimed to provide industrial technology developers, suppliers and practitioners with valuable, readily usable information and tools aimed towards considering MDC as an alternative, more energy efficient and sustainable hypersaline brine treatment process towards achieving zero liquid discharge.

Acknowledgements

The project team wishes to thank the Water Research Commission for the funding and support towards this project. In particular, Prof John Ngoni Zvimba and Mr Benny Mokgonyana.

In addition, we would like to express our sincere appreciation for the guidance received from the following reference group members:

Prof John Ngoni Zvimba	:	Water Research Commission (Chairman)
Dr Enos Sitabule	:	Sasol Technology
Prof Johannes Sekomeng Modise	:	Vaal University of Technology
Mr Achim Wurster	:	Water Treatment Process Engineering
Dr Lynette Mariah Baratta	:	SASOL Technology
Dr Parani Sundararajan	:	University of Johannesburg
Prof Craig Sheridan	:	University of the Witwatersrand
Prof Lingam Visvanathan Pillay	:	University of Stellenbosch
Dr Gerhard Gericke	:	Independent

Table of Contents

Executive Summary	III
Acknowledgements	VI
Table of Contents	VII
List of Figures	IX
List of Tables	XI
CHAPTER 1 Introduction and Background	1
CHAPTER 2 Literature Review.....	4
2.1 Water Treatment Processes in General.....	4
2.2 The Generation of Brine and Brine Treatment Options.....	4
2.3 Membrane Distillation Crystallisation (MDC)	5
2.3.1 Types of Membrane Distillation	7
2.4 Membrane Distillation Crystallisation Process Parameters	9
2.4.1 Heat and mass transfer.....	9
2.4.2 Temperature	12
2.4.3 Feed concentration.....	12
2.4.4 Flow rate.....	13
2.4.5 Fouling	13
2.5 Key Membrane Characteristics for Membrane Distillation	13
2.5.1 Polymer type and its intrinsic properties.....	14
2.5.2 Wetting resistance or Liquid Entering Pressure (LEP)	15
2.5.3 Membrane thickness.....	17
2.5.4 Membrane pore size and pore distribution	18
2.5.5 Membrane porosity.....	19
2.5.6 Tortuosity.....	19
2.5.7 Backing structures	19
2.5.8 Mechanical Strength	20
2.5.9 Cost of production of membranes.....	20
CHAPTER 3 MDC Experimental Set Up and Methodology.....	22
3.1 Experiment set-up.....	22
3.2 Experimental Methodology.....	28
3.2.1 DCMD equipment testing methodology	28
3.2.2 Measurement of experimental variables and data logging methodology	30
3.2.3 Experimental procedure.....	30
3.3 Selection of model brines for the study.....	31
3.4 Selection of key membrane characteristics to be investigated	33
3.4.1 Hydrophobicity	33
3.4.2 Membrane Thickness	33
3.4.3 Membrane Porosity	33
3.4.4 Membrane Pore Size	34

CHAPTER 4	Establishing the minimum acceptable flux for MDC and development of a flux prediction model for MDC	35
4.1	Establishing the minimum acceptable flux for MDC	35
4.1.1	Experimental Methodology.....	35
4.1.2	Results and Discussion.....	35
4.2	Development of a flux prediction model for MDC	37
4.2.1	Experimental Methodology.....	37
4.2.2	Results and Discussion.....	38
CHAPTER 5	Investigating the effect of membrane characteristics on MD performance for Type 2 prepared brine and real world industrial brine	45
5.1	Investigation on Type 2 Prepared BrinPe	45
5.1.1	Experimental methodology for investigation on Type 2 prepared brine	45
5.1.2	Results and discussion on the investigation on the effect of membrane characteristics on MD performance for Type 2 prepared brine.....	46
5.2	Investigation on real-world industrial brine	49
5.2.1	Experimental methodology for investigation using real-world industrial brine	49
5.2.2	Results and discussion on the effect of pore size on the performance of MD using real industrial brine emanating from an RO process.....	50
CHAPTER 6	Scaling/fouling effects on MD performance and the development of an algorithm to determine the suitability of MD for the treatment of brines.....	52
6.1	Scaling/fouling effects on MD performance.....	52
6.1.1	Scaling/fouling effects on MD performance for prepared Type 1 brine.....	52
6.1.2	Scaling/fouling effects on MD performance for Type 2 prepared brine.....	55
6.1.3	Effect of particle size on the scaling/fouling effects on MD performance for Type 2 prepared brine.....	61
6.2	Development algorithm to determine membrane distillation suitability towards brine treatment	63
CHAPTER 7	Conclusions and Recommendations.....	64
REFERENCES	67

List of Figures

Figure 1: Schematic of a typical membrane crystallisation unit (Pantonja, 2016)	6
Figure 2: Summary of Different Membrane Distillation Configurations (EMIS, 2010).....	9
Figure 3: DCMD heat and mass transfer through membrane (Camacho et al., 2013)	10
Figure 4: General configuration of the DCMD experimental set up	25
Figure 5: Membrane element cell assembly of the DCMD experimental set up.....	26
Figure 6: Photograph of commissioned DCMD experimental set up.....	27
Figure 7: Photograph of commissioned DCMD experimental set up.....	28
Figure 8: Cost of MD for treating highly saline brines	36
Figure 9: 3-dimensional representation of the effect of a variation in the feed temperature and feed concentration on the change in flux for Type 1 brine using the 0.22 μm membrane pore size.....	38
Figure 10: 3-dimensional representation of the effect of a variation in the feed temperature and feed concentration on the change in flux for Type 1 brine using the 0.45 μm membrane pore size.....	38
Figure 11: Change in flux rate with a change in feed temperature at different feed concentration levels for the treatment of Type 1 brine using the 0.22 μm membrane pore size.....	39
Figure 12: Change in flux rate with a change in feed temperature at different feed concentration levels for the treatment of Type 1 brine using the 0.45 μm membrane pore size.....	40
Figure 13: Normal plot of residuals for Type 1 brine flux model	42
Figure 14: Predicted values vs Actual values.....	43
Figure 15: Perturbation plot of factor interaction for GVHP membrane for the treatment of Type 1 brine	44
Figure 16: Effects of feed temperature on flux rate for the treatment of prepared Type 1 brine (Initial feed TDS 11870 mg/L) using a 0.22 μm and 0.45 μm pore size membrane	47
Figure 17: Effects of feed concentration and suspended solids for the treatment of prepared Type 2 brine using 0.22 μm (GVHP) and 0.45 μm (HVHP) membrane pore size	48
Figure 18: Effects of time (increase in feed concentration and suspended solids) on the water recovery and salt rejection for the treatment of prepared Type 2 brine using 0.22 μm (GVHP) and 0.45 μm (HVHP) membrane pore size	49
Figure 19: Feed and permeate conductivity as a function of recovery for (6-hour run, 200 g/L initial TDS) prepared Type 1 brine using 0.22 μm pore size and 0.45 μm pore size membranes.....	53
Figure 20: Effects of concentration on flux rate for the treatment of Type 1 brine.....	54
Figure 21: Flux rate and TSS as a function of water recovery for prepared Type 2 brine using the 0.22 μm pore size membrane	56
Figure 22: Flux rate and TSS as a function of water recovery for prepared Type 2 brine using the 0.45 μm pore size membrane	57
Figure 23: Permeate conductivity and TSS as a function of water recovery for prepared Type 2 brine using the 0.22 μm pore size membrane	58
Figure 24: Permeate conductivity and TSS as a function of water recovery for prepared Type 2 brine using the 0.45 μm pore size membrane	58
Figure 25: Salt rejection and TSS as a function of water recovery for prepared Type 2 brine using the 0.22 μm pore size membrane.....	59

Figure 26: Salt rejection and TSS as a function of water recovery for prepared Type 2 brine using the 0.45 μm pore size membrane	60
Figure 27: Permeate flux vs Suspended solids in solution	60
Figure 28: Effect of particle size on the flux rate for prepared Type 2 brine using 0.22 μm pore size and 0.45 μm pore size membranes.....	62
Figure 29: MD Algorithm	63

List of Tables

Table 1: Experimentally determined membrane properties	15
Table 2: Typical commercial flat sheet membranes commonly used in MD (Khayet, n.d.)	16
Table 3: Membrane thickness from various membrane polymers used	17
Table 4: Young modulus for different membrane types	20
Table 5: Direct Contact Membrane Distillation set up key equipment components and their specific function.....	24
Table 6: Composition of synthetic Type 1 brine NaCl concentration levels used in this study	31
Table 7: Chemical make-up of synthetic coal mine brine	32
Table 8: Chemical make-up of the desupersaturated synthetic coal mine brine that was treated with RO (stage two RO)	32
Table 9: Merck Millipore GVHP and HVHP membrane characteristics	34
Table 10: Type 1 Brine NaCl concentration levels used	37
Table 11: Experimental matrix using response surface approach	37
Table 12: ANOVA response for the Quadratic model using Design Expert 11 for Type 1 brine	41
Table 13: Experimental matrix used to investigate the effect of membrane characteristics on MD performance for Type 2 brine	45
Table 14: Summary of experimental run results of the prepared Type 2 brine	46
Table 15: Water analysis data for the real brine emanating from industrial wastewater used for Experiment 7.....	50
Table 16: Scaling indices for real brine used in Experiment 7	50
Table 17: Results for real brine after running system for 480 minutes	51
Table 18: Experimental Matrix.....	52
Table 19: Type 1 Brine (NaCl) concentration level used.....	52
Table 20: Permeate flux rate of Experiment 4 to determine the effect of scaling/fouling for prepared Type 1 brine	53
Table 21: Summary of results for scaling/fouling experiments using the prepared Type 2 brine	56

This page was intentionally left blank

1 Introduction and Background

The generation of brine waste streams emanating from water treatment processes such as reverse osmosis (RO), multi-stage flash (MSF) and multi-effect distillation (MED) are a major concern for the environment. A 2019 global outlook study (Jones et al., 2019) revealed that there are 15906 operational desalination plants globally, producing around 142 million m³/day of brine. Reverse osmosis (69%), multi-stage flash (18%) and multi-effect distillation (7%) account for 94% of the total hypersaline brine volumes generated globally.

The aqueous characteristics of these hypersaline brines can generally be classified into two main categories: (i) monovalent ion dominant, non-scaling brines, e.g. sodium chloride dominant brines emanating from seawater desalination processes and (ii) divalent and trivalent ion dominant brines with scaling and/or fouling potential, e.g. brines emanating from the desalination of brackish water.

Brine waste-handling and disposal methodologies are largely contingent on the geography in the vicinity of the plant generating the brine and include discharge into oceans, inland water bodies such as rivers, surface dams and sewers, as well as deep-well injection and brine storage in waste evaporation ponds. These methodologies are not environmentally sustainable and consequently, brine treatment towards achieving minimal liquid discharge (MLD) or ultimately zero liquid discharge (ZLD) in a cost-effective way has become a major challenge. In most cases, although the first 90-95% of the waste stream can be treated relatively cost-effectively using well-established, conventional, commercially available technologies, the capital equipment costs and operating costs associated with treating the remaining 5% using conventional thermal evaporation process typically tends to double the overall treatment cost.

Emerging technologies under investigation for the treatment of brines include forward osmosis (FO), eutectic freeze crystallisation (EFC), osmotically assisted reverse osmosis (OARO) and membrane distillation crystallisation (MDC).

Membrane Distillation Crystallisation (MDC) offers a sustainable wastewater treatment option for saline and hypersaline effluent streams. This is particularly so when utilising excess waste heat from peripheral processes to produce pure water because MDC requires significantly lower operating temperatures (60-80°C). Furthermore, MDC systems can be constructed from less expensive materials owing to the requirement for lower hydrostatic operating pressures when compared to using high pressure reverse osmosis or the need for exotic materials of construction due to increased corrosion rates at higher operating temperatures as is the case for conventional evaporators. In addition to this, the generation of potentially usable salts using MDC converts a waste effluent stream into one with saleable products of value that can either be reused, recycled, or sold to offset water treatment costs towards driving down the unit cost per m³ of treated water.

Other advantages of MDC include: a reduction in membrane fouling when compared to other pressure driven processes, improved rejection factors for feed streams containing non-volatile solutes and the ability to treat high total dissolved solids (TDS) feed solutions that are close to their saturation limit (Qtaishat

& Banat, 2012). Furthermore, when applied to the treatment of acid mine drainage (AMD), the MDC process is able to operate in very acidic or basic streams (Zeng & Gao, 2010), thus the AMD streams would not necessarily need to be pre-treated or neutralized pre-MDC process.

Some disadvantages identified with MDC include:

- Limited commercial production capacity of MDC specific hydrophobic membranes for use in industrial scale continuous MDC processes
- The prohibitive cost of commercial membrane modules owing to absence of the typical manufacturing cost savings that stem from manufacturing at scale in the presence of significant demand and supply drivers
- Risks associated with membrane wetting due to the variability in the hydrophobic nature of the produced membranes
- The apparent historically low membrane flux, resulting in requirement for large membrane surface areas when compared to other membrane treatment processes

All of these disadvantages may largely be attributed to the lack of research to date, specifically in the design of MDC membranes (Khayet, n.d.).

During MDC, the membrane distillation MD aspect of the process is used to concentrate a stream to a level of supersaturation where salt(s) begin to crystallise out in a crystalliser (Tun et al., 2005). Numerous researchers have investigated the use of MDC for the treatment of diverse industrial wastewater streams but the application of MDC specifically to the treatment of mine wastewaters is especially limited. Furthermore, a review by Alkudhiri et al. (2012) found that the application of MDC to different industrial streams is still limited. In addition, there is a considerable deficiency in the research surrounding the influence of high salt concentrations in the feed on the efficiency of the MD process (Alkudhiri et al., 2012).

The use of MDC for the treatment of mine wastewater has not been a major focus of research even though there is great potential in this field. MDC has the potential to treat concentrated water solutions beyond the operational capabilities of RO processes. Despite the potential advantages and applicability of the technology, the MDC process is yet to be commercially readily accessible and applied within the broader industrial scale. In order to realise this potential, there are some technological challenges that need to be overcome, the most significant of which is ease of accessibility, availability and scalability of MD specific membranes. Most of the membranes currently being used are not specifically designed for MD processes. In addition to this, these membranes are too expensive for commercial viability and have limited scalability for large-scale applications owing to the inability to seal and compact them into modules. This is exacerbated by their low mechanical strength, particularly in the absence of supporting/backing layers.

The development of an MDC process also requires better crystalliser control strategies, particularly in terms of the control of particle formation mechanisms since most MDC research is currently based on a batch process, thereby limiting the crystalliser control (Tun et al., 2005).

The WRC Project K5/2223//3 showed how the temperature and concentrations of the feed and product solutions affected the flux through the membrane, however the effect of the membrane characteristics on the flux and the effects of scaling/fouling was not investigated. Furthermore, results from the WRC Project K5/2223//3 indicated that a flux of up to 65 L/m²-hr could be achieved, which is up to 3 times higher than those found previously in literature, therefore suggesting a definite possibility that membrane distillation has the potential to be used to increase water recovery from RO brines whilst generating usable salts as by-products.

The aims and objectives of this study were to identify quintessential considerations, mainly related to key membrane characteristics and performance criteria, when assessing the viability of implementing and selecting MDC over alternative technologies. Specifically, the study focussed on:

- i) Determining the minimum acceptable flux below which membrane distillation as an emerging technology becomes commercially unviable relative to existing commercial brine treatment technologies
- ii) Development of a flux prediction model that uses brine salinity, feed temperature and membrane pore size as input variables to yield the predicted flux as the response variable. The utility in this model lies in its ability to quickly ascertain whether any specific brine under consideration meets the minimum acceptable flux criterion described in (i) above
- iii) Development of a decision-making tool for industrial practitioners to ascertain whether membrane distillation is a suitable alternative for the treatment of hypersaline brines and furthermore to provide operating parameter guidelines for a specific brine being investigated based on its aqueous and scaling characteristics.

Using the information obtained from the experimental investigations and the decision-making tool developed, prospective users of membrane distillation technology would be better informed in assessing the viability of using membrane distillation for brine treatment. Furthermore, the decision-making tool provided guidelines in terms of membrane selection and process operating conditions for specific types of brines.

This study aimed to provide industrial technology developers, suppliers and practitioners with valuable, readily usable information and tools aimed towards considering MDC as an alternative, more energy efficient and sustainable hypersaline brine treatment process towards achieving zero liquid discharge.

2 Literature Review

2.1 Water Treatment Processes in General

Wastewater is typically characterised as containing elevated levels of suspended solids and dissolved species. Treatment of wastewater is usually carried out in a multi-stage process before it can be discharged or reused. Larger particles and coarse solids in the wastewater are removed in a pre-treatment processes such as screening in order not to block up or cause damage to equipment in any subsequent downstream treatment processes.

Smaller sediment particles may be removed by gravity settling, flotation, filtration (both multi-media and membrane processes) or by skimming, amongst others, during the primary treatment process. The efficiency of the solid-liquid separation process can be enhanced by the addition of coagulants and flocculants. For dissolved organic compounds in the wastewater, a biological process can be used during secondary treatment to remove the organics and suspended solids. Any further constituents in the wastewater that are not removed by the secondary processes require individual treatment processes during the tertiary or advanced processes such as reverse osmosis.

When looking specifically at the treatment of industrial and mine wastewaters, these are typically characterised as having elevated levels of inorganic and organic suspended and dissolved material and variable salinity. Although the general treatment process for these types of industrial and mining waters may be similar to other types of wastewater, the presence of metals as well as a dynamic variability in the feed water composition adds further complexity to the treatment process. Typically, the treatment process ensures the removal of fines and suspended solids, followed by the removal of dissolved ionic species sometimes including metals using the appropriate technologies (pH-driven chemical softening, heavy metal precipitation followed by ultrafiltration (UF) and reverse osmosis (RO)), in order to achieve the final product water quality specification required.

2.2 The Generation of Brine and Brine Treatment Options

Desalination processes such as RO and thermal evaporation are predominantly used for the removal or reduction of dissolved ionic species. Currently, RO is still considered to be the most cost-effective method of desalination to remove dissolved ionic species and reduce salinity.

However, the reject or retentate from these RO processes, referred to in the context of this study as brine, continues to pose both technical, environmental and economic challenges towards achieving sustainable zero liquid discharge (ZLD) scenarios.

Some common brine treatment and disposal methods include: Direct surface water discharge, discharge to a sewage treatment plant, deep well injection, evaporation ponds, brine concentrators/Zero liquid discharge, mixing with cooling water discharge, mixing with sewage treatment

effluent, electro-dialysis and Vibratory Shear Enhanced Processing (VSEP) Membrane System (Balasubramanian, 2013). Many of these may not be feasible due to environmental and geological impacts to the area. Importantly, the brine may still contain reusable salts and therefore the management of the brine is an integral part of the process.

This project focuses on membrane distillation (MD) as a brine treatment and/or concentration method. The maximum achievable recovery is limited in an RO process by membrane scaling/fouling at concentrations beyond the maximum antiscalant tolerance levels as well as the osmotic pressure limitation. Since precipitation within the RO element is to be avoided, MD could be applicable in zero (or near zero) liquid discharge applications as relatively high fluxes can be obtained at salt concentrations higher than are allowable for a RO application.

The MD process is a thermally driven separation process that only allows vapour molecules to be transported across a microscopic, hydrophobic membrane, without altering the vapour equilibrium of the different components in the process liquids. The process is driven by the vapour pressure differences across the membrane rather than a pressure gradient (Curcio & Drioli, 2005). The trans-membrane temperature differential (ΔT) creates a vapour pressure gradient for separation, whilst the hydrophobic microporous membrane separates the heated feed from the cooled receiving phase, allowing only volatile compounds to pass through, with the process liquid being in contact with at least one side of the membrane (Alkudhiri et al., 2012; Camacho et al., 2013).

The MD process relies on a highly hydrophobic micro-porous membrane to maintain a liquid-vapour interface and to only allow water in the vapour state to pass through. Since MD is driven thermally, it is less sensitive to the feed concentration compared to alternative pressure driven membrane separation processes that are often limited to a maximum dry matter content of 12-20% (Ramirez et al., 2006). Other advantages of MD include a theoretical complete rejection of non-volatile components, low operating pressure, reduced vapour space compared to conventional distillation and evaporation processes, and low operating temperatures of the feed (Tomaszewska, 2000).

2.3 Membrane Distillation Crystallisation (MDC)

Recent advances in MD, which previously focussed primarily on the recovery of water, have led to the extension of this process to the crystallisation stage as a means of recovering some value from the dissolved species in the form of reusable/saleable salts, hence, the extension of MD to Membrane Distillation Crystallisation (MDC) to include the crystallisation aspects. The MDC process is a hybrid membrane separation-crystallization process whereby the brine sequentially becomes saturated, then supersaturated at which point crystallisation of the salts that have exceeded their equilibrium solubility limit takes place and these crystals are then collected/harvested in an external crystallizer (Susanto, 2011).

Membrane crystallisation (MCr) was previously introduced by Curico et al. (2001) based on investigations to produce high quality crystals from solutions. The advantages of this technique become evident when

comparing it to conventional crystallisation techniques such as the circulating-magma crystalliser. In the latter case, solvent evaporation and solute crystallisation occur in the same place. This results in temperature gradients between the surface and the bulk of the body, often compromising the suspension uniformity of the crystalline products (Curcio et al., 2001). In MDC however, these two phenomena occur in separate reactors – the solvent evaporation occurs within the MD module whereas the crystallisation takes place in a separate crystalliser. Furthermore, membrane crystallisers functioning under forced solution flow conditions are characterised by an axial flux in the laminar regime of the crystallising solution through the membrane fibres (Curcio & Drioli, 2005). This apparently induces a well-organised orientation of the particles, resulting in crystals with improved quality and size distribution, which is important when crystals need to undergo further treatment or reactions (Curcio & Drioli, 2005).

The method is useful especially when crystals of non-volatile electrolytes are to be recovered. In this hybrid separation process, the pure solvent (from the permeate side) and the high quality crystal product (from the retentate flow circulated back to the crystallizer) are obtained simultaneously. The method has exhibited several advantages over other treatment technologies such as lower energy consumption, low cost, high efficiency and being environmentally friendly. The process has potential for use in several industrial applications and is not restricted to wastewater treatment. Figure 1 illustrates a typical MDC process configuration that is used to recover the crystalline salts:

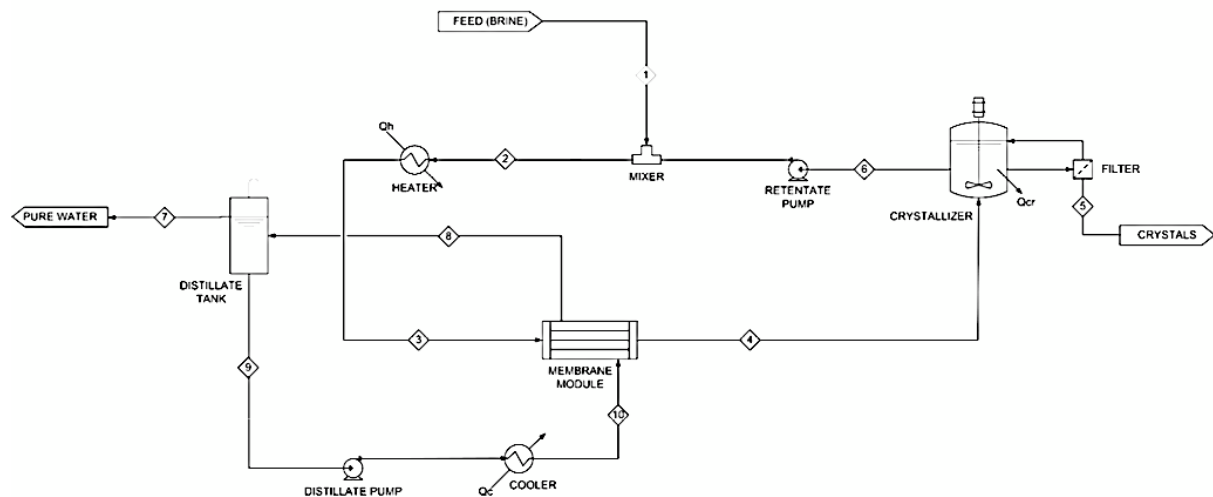


Figure 1: Schematic of a typical membrane crystallisation unit (Pantonja, 2016)

With an MDC process (such as in the Direct Contact Membrane Distillation (DCMD) configuration), the warm brine (retentate) flows counter current to the cold distillate (pure water). A microporous hydrophobic membrane in the form of capillary tubes separates the two streams. The continual removal of water from the retentate increases the concentration and supersaturation of various species in the

mother liquor, thereby driving the initiation of nucleation and crystal growth in the crystalliser. Ideally, the crystallisation process is controlled such that bulk of the crystal formation is isolated to the crystalliser so as to minimise crystal deposition on the membrane, which would result in membrane scaling/fouling and blocking of the membrane pores, consequently resulting in a major deterioration in system performance. One of the operational strategies (at least for salts that do not exhibit an inverse solubility, e.g. gypsum) is to ensure that the solution flowing through the membrane is always at a temperature high enough to maintain under saturation conditions, while the crystalliser is operated at a lower temperature, which promotes tank maintains a temperature which favours crystal formation.

The maximum achievable recovery is limited in an RO process by membrane scaling/fouling at concentrations beyond the maximum antiscalant tolerance levels as well as osmotic pressure limitations. Since precipitation within the RO element is to be avoided, MD could be applicable in zero (or near zero) liquid discharge applications seeing as relatively high fluxes can be obtained at salt concentrations higher than are allowable for a RO application.

However, this requires proper management of precipitating salts to avoid membrane fouling, which is significantly less detrimental to the membrane given that the scaling/scaling does not occur at elevated pressures, as would be the case in a RO process. One way of managing these salts is with MD crystallisation. This method has been explored for NaCl and Na₂SO₄ solutions, where it was found that at certain feed concentrations the flux declines due to crystal formation on the membrane surface. This, in turn, reduces the membrane's salt rejection characteristics because salts can penetrate into the pores. Using MD together with MD crystallisation allows for an improved separation of salts from solution and this concept has the potential to expand into other industries, such as drug development (Camacho et al., 2013).

2.3.1 Types of Membrane Distillation

There are four categories of MD that differ based on how the permeate is processed. These categories are described below and can be seen in Figure 2 (Salehi & Rostamani, 2013; Camacho et al., 2013):

(a) Sweep Gas Membrane Distillation (SGMD):

In Sweeping Gas Membrane Distillation (SGMD) the vapour produced on the product side of the membrane is stripped with an inert gas which flows to a condenser where the liquid is collected (Figure 2a). The flowing gas improves the mass flux by reducing the boundary layer resistance. This type of distillation is particularly suitable for the removal of volatiles from an aqueous solution (Walton, 2000). An underlying disadvantage of the method is that only a small volume of the permeate diffuses into the large sweep gas volumes, requiring a large condenser.

(b) Air Gap Membrane Distillation (AGMD):

Air Gap Membrane Distillation (AGMD) has the feed liquid in contact with the membrane while there is an air gap between the membrane and the condensation surface on the product side. This setup has the highest energy efficiency due to a decrease in heat transfer from the feed to

the product, but at the same time, the air gap results in a lower flux. This type of distillation is particularly suitable for systems that have low energy requirements and is suitable for most MD applications such as desalination (Banat & Simandi, 1998; Walton, 2000) and the extraction of most volatile compounds from aqueous solutions (Payo, 1999). A typical AGMD configuration is illustrated in Figure 2b.

(c) Vacuum Membrane Distillation (VMD):

In Vacuum Membrane Distillation (VMD) the product side of the membrane is vapour or air under reduced pressure, thereby creating a vacuum that removes trapped gas in the pores and improves the mass flux. The permeate gas can then be condensed to obtain the product. The heat loss by conduction is negligible, which adds to the advantage of the method. This method of distillation is also particularly suitable for the removal of volatiles from an aqueous solution, although the energy costs to create the vacuum are high (Bandini & Sarti, 1999). A typical VMD configuration is illustrated in Figure 2c.

(d) Direct Contact Membrane Distillation (DCMD):

Direct Contact Membrane Distillation (DCMD) is the simplest and most commonly used configuration for membrane distillation. Illustrated in Figure 2d, both sides of the membrane are in contact with the hot and cold fluid, producing reasonably high flux but also resulting in low energy efficiency due to the high heat loss through conduction to the permeate side. In this type of configuration, the vapour is transferred from the feed side to the permeate side by a pressure difference across the membrane. The membrane is hydrophobic, which does not allow the feed to diffuse across the membrane and only allowing the vapour to pass through. This type of distillation is best suited to concentrated aqueous solutions, chiefly in food industries (Alves & Coelho, 2006; Gunko et al., 2006) and desalination (Hsu et al., 2002).

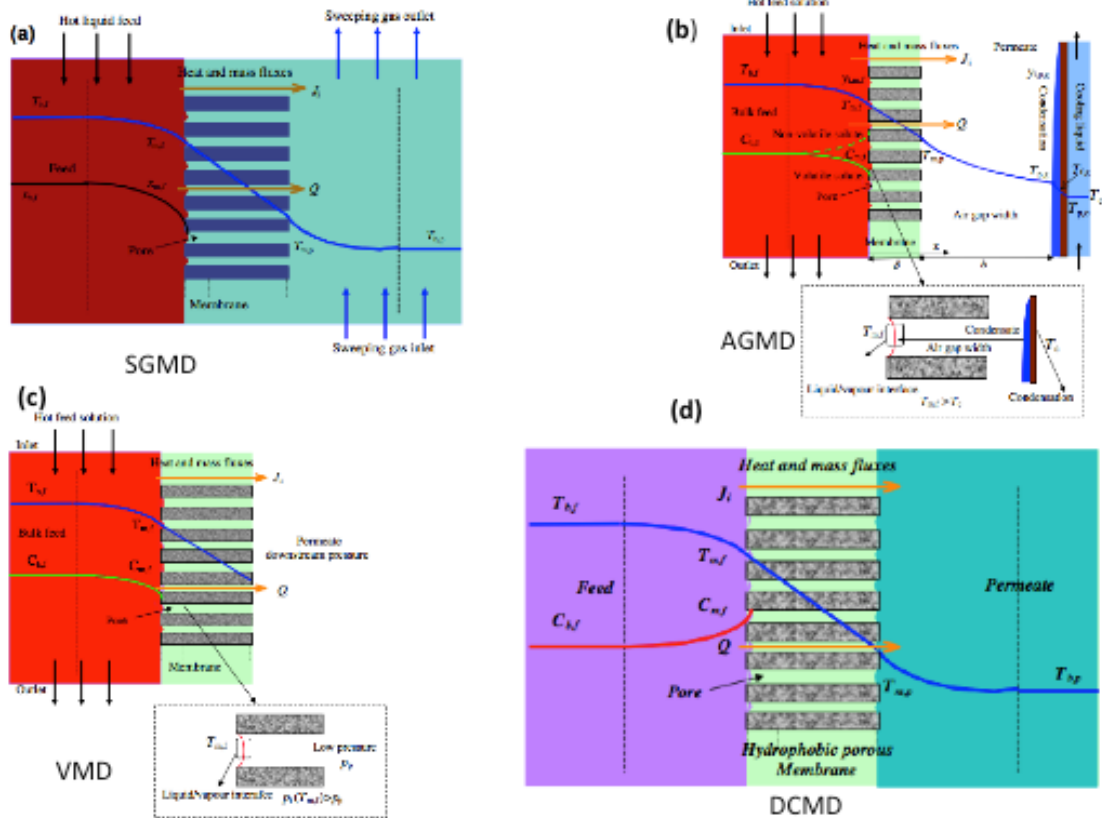


Figure 2: Summary of Different Membrane Distillation Configurations (EMIS, 2010)

2.4 Membrane Distillation Crystallisation Process Parameters

The two main underlying phenomena that govern the efficiency of a MDC process are the heat and mass transfer of the system; these are discussed below along with other parameters that affect a MDC process.

2.4.1 Heat and mass transfer

Heat and mass transfer are coupled in MD, resulting in complex performance characteristics that are challenging to optimize (Qtaishat et al., 2007). The typical heat and mass transfer characteristics of a DCMMD process are illustrated in Figure 3.

The mass transfer in the MD process can also be divided into three stages: (a) Transport across the polarisation layer in the feed stream; (b) Diffusive transport of vapour through the membrane driven by the vapour pressure differential; (c) Condensation into the cold stream on the permeate side and diffusion into the permeate bulk stream (Hausmann, 2013).

The vapour is transferred by convection and diffusion through the microporous membrane at a flux (J_w), which is dependent on the membrane characteristics and the driving force. Equation 1 represents the mass flux.

$$J_w = C_w \Delta P_m \quad (1)$$

Where C_w is the overall mass transfer coefficient and ΔP_m is the vapour pressure difference between the feed and product sides, denoted as $\Delta P_m = P_{mf} - P_{mp}$ (KHALIFA, A. E. and Lawal, D. U., 2014).

From Figure 3 it can be seen that heat is transferred in three stages: (a) Transfer from the bulk feed solution (T_{FB}) to the membrane surface (T_{FM}); (b) Transport across the membrane, through evaporation and convective transport, as water evaporates and is transported across the membrane from the liquid-vapour interface at the pore entrance. Conductive heat transfer also takes place through the membrane matrix and the gas filled pores; (c) Condensation of the water at T_{PM} on the permeate side. The cold flow temperature increases across the permeate side boundary layer to the permeate bulk temperature (T_{PB}) (Curcio & Drioli, 2005; Burgoyne & Vahdati, 2000; Qtaishat et al., 2007). As can be seen, the flux for both the mass and heat is from the heated feed side to the cold product side. The feed temperature T_{FB} decreases through the boundary layer to T_1 at the feed membrane wall, whereas the product temperature T_{PB} increases to T_2 at the product membrane wall. Water from the feed evaporates at T_1 , is transported across the membrane, condenses at T_2 and is absorbed by the cold product flow. This process therefore results in the transfer of heat via convection from the feed to the feed side membrane wall and, similarly, from the product side membrane wall to the product. Additionally, conductive heat transfer takes place through the membrane wall and stagnant gas/vapour in the membrane pores via sensible heat, while latent heat is transferred from the feed to the product by the vapour (Camacho et al., 2013).

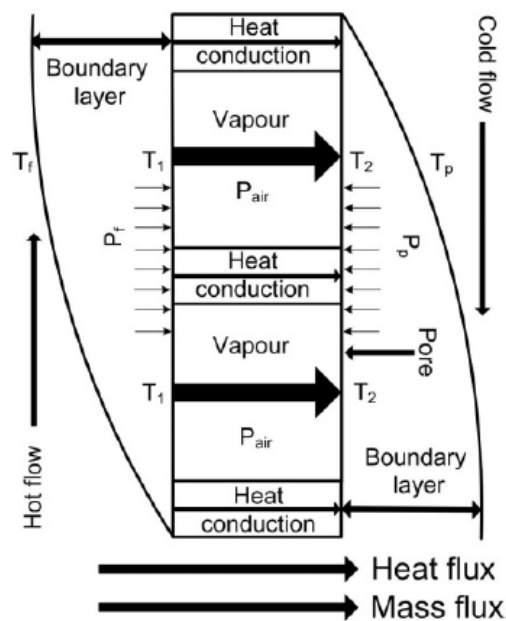


Figure 3: DCMD heat and mass transfer through membrane (Camacho et al., 2013)

The mass transfer in the MD process can also be divided into three stages: (a) Transport across the polarisation layer in the feed stream; (b) Diffusive transport of vapour through the membrane driven by the vapour pressure differential; (c) Condensation into the cold stream on the permeate side and diffusion into the permeate bulk stream (Hausmann, 2013).

The vapour is transferred by convection and diffusion through the microporous membrane at a flux (J_w), which is dependent on the membrane characteristics and the driving force. Equation 2 represents the mass flux.

$$J_w = C_w \Delta P_m \quad (2)$$

Where C_w is the overall mass transfer coefficient and ΔP_m is the vapour pressure difference between the feed and product sides, denoted as $\Delta P_m = P_{mf} - P_{mp}$ (KHALIFA, A. E. and Lawal, D. U., 2014).

Vapour pressure is the pressure exerted by a vapour in thermodynamic equilibrium with its condensed phase at a given temperature in a closed system. The two factors affecting vapour pressure are temperature and the type of liquid. There are a number of methods by which the vapour pressure is correlated as a function of temperature. These are mainly derived from the Clausius Clapeyron equation given in Equation 3:

$$\ln(P^{sat}) = \ln(A) - \frac{\Delta H_{vap}}{RT} \quad (3)$$

From this, Antoine's equation was developed as in Equation 4:

$$\ln(P^{sat}) = A + \frac{B}{T+C} \quad (4)$$

This equation is used mainly for low to moderate vapour pressures and does not fit data accurately above the normal boiling point. Consequently, the modified Riedel equation was developed as given in Equation 5. Although the constants have been determined for a wide variety of chemicals, for the purposes of this study only the constants specific to water are of interest. The water specific equation is given as Equation 6 (Liley et al., 1999):

$$\ln(P^{sat}) = A + \frac{B}{T} + C \ln T + DT^E \quad (5)$$

$$\ln(P^{sat}) = 73.649 - \frac{7258.2}{T} - 7.3037 \ln T + 4.1653 \times 10^{-6} \times T^2 \quad (6)$$

Referring to Figure 3, the driving force of the vapour transfer rate is the difference in vapour pressure at T_2 and T_1 , not the bulk temperatures of the feed and product (T_f and T_p). At the bulk feed and product temperatures the driving force would be overestimated with a greater vapour pressure difference. The permeability of the membrane also affects the transfer rate. Due to the evaporation at the feed

membrane wall, the feed vapour concentration increases from the feed C_f to the feed membrane wall C_i .

The ratio of the difference between the membrane wall temperatures and the bulk feed and product temperatures is known as temperature polarization, TP (Camacho et al., 2013).

$$TP = \frac{T_1 - T_2}{T_f - T_p} \quad (7)$$

From Equation 7 it can be seen that the ideal TP would be when the membrane wall temperatures are equal to their respective bulk fluid temperatures (TP = 1). This would result in a greater difference in the vapour pressures, thereby increasing the flux across the membrane. In order to achieve a TP of 1, the temperature gradient in the thermal boundary layer needs to be decreased. This can be done by enhancing the turbulence of the stream by either increasing the flow rate or inserting turbulence promoters. However, the relationship between turbulence and flux is not proportional, as beyond a certain level of turbulence, its effect on flux decreases. Therefore, an optimal flow rate has to be determined for a system to reduce the energy cost of pumping while still achieving a high flux rate (Camacho et al., 2013).

Additionally, if the membrane is compressible, the increase in flux due to higher turbulence will be negated by an increase in pressure, due to the square relationship between hydrostatic pressure and the flow rate (Camacho et al., 2013).

2.4.2 Temperature

An increase in feed temperature will result in a greater vapour pressure differential, which, in turn, increases the mass flux through the membrane.

On the other hand, there will be increased heat loss in the system considering conductive heat loss and the temperature difference is directly proportional. Both of these factors also result in an increase in the TP effect (Camacho et al., 2013).

Conversely, an increase in the permeate temperature will result in decreased mass flux due to the decrease in the vapour pressure differential. A decrease in the permeate temperature should have a smaller increase in the flux than an increase in the feed temperature because of the exponential increase in the vapour pressure with temperature.

2.4.3 Feed concentration

Variability in the concentration of solutes in a solvent affects the vapour pressure, which for the purposes of this study is the concentration of salt in water. Raoult's law can be used to approximate the vapour pressure of dilute solutions with Equation 8 (Van Ness & Abott, 1999):

$$P^{Sat} = X_{solv} \times P_{solv}^0 \quad (8)$$

Where P^{Sat} is the vapour pressure of the solution, X_{solv} is the mole fraction of the solvent and P_{solv}^0 is the vapour pressure of the pure solvent at a particular temperature.

From Equation 8 an increase in feed concentration results in a decrease in vapour pressure of the solution and, by extension, a decrease in permeate flux since vapour pressure is the driving force. Furthermore, an increase in feed concentration leads to an increased viscosity of the solution. This would yield a smaller Reynolds number, indicating less turbulent flow and lead to a decrease in mass flux.

2.4.4 Flow rate

An increase in feed flow rate results in a decrease in the thermal boundary layer, thereby reducing the effect of temperature polarisation and improving the mass flux. However, an increase in flow rate also leads to increased hydrostatic pressure, which could lead to membrane pore wetting if the liquid entry pressure (LEP) is exceeded (Onsekizoglu, 2012). An increase in permeate side flow rate, similarly, results in a reduced TP effect.

2.4.5 Fouling

Fouling will reduce the effective membrane area and therefore result in a decrease in mass flux. Furthermore, due to the reduced flow there will also be an increase in temperature polarisation effect. Fouling may also introduce wettability of the pores, thereby allowing solutes to pass through the membrane (Gryta, 2001)

2.5 Key Membrane Characteristics for Membrane Distillation

The following characteristics are viewed as key to the performance of MD membranes:

- i. **Hydrophobicity** – membranes should be hydrophobic or have at least one hydrophobic layer
- ii. **Pore size and porosity** – membranes should be microporous
- iii. **Membrane thickness and tortuosity** – membranes should have low resistance to mass transfer
- iv. **Thermal characteristics** – membranes should have low thermal conductivity to prevent heat loss across the membrane and should exhibit good thermal stability in extreme temperatures
- v. **Chemical stability** – membranes should have a high resistance to chemicals, such as acids and bases

Hydrophobic microporous membranes that were initially developed for microfiltration applications are typically used in most commercial MD system applications. However, these membranes are not optimized for the MD process (Eyekens, 2016(2), Teoh, 2009; Boyandi, 2009). Consequently, further optimisation of these repurposed membranes specifically for application in an MD process could greatly enhance the MD process.

The type of membrane and its characteristics influences the efficiency and operation of the membrane. A correlation between trans-membrane flux and membrane characteristics is given by the following relationship (Kullab, 2011):

$$N \propto \frac{r^a \varepsilon}{\tau \delta_m} \quad (9)$$

Where r is the average pore size for Knudsen diffusion ($a = 1$) or the average squared pore size for viscous flux ($a = 2$), ε is the membrane porosity, τ is the membrane tortuosity, and δ_m is the membrane thickness.

Reviews by Lawson and Lloyd (1997) have suggested general considerations of typical membrane characteristics such as liquid entering pressure (LEP), membrane thickness, membrane porosity and tortuosity, membrane pore size and distribution, which essentially affect membrane performance and transmembrane flux. The following sections describe the effect of the various membrane characteristics on the performance of MD and the recent findings:

2.5.1 Polymer type and its intrinsic properties

Many membranes applied either on pilot scale or commercial scale are made of one of the following materials: Polytetrafluoroethylene (PTFE), Polyvinylidene fluoride (PVDF), or polypropylene (PP). The polymers have a great wetting resistance due to the low surface tension on the surfaces. Recently, Polyethylene (PE) and modified Polyether sulfone (PES) membranes are becoming common commercial membranes and are currently being explored for their application in MD [Eyekens, 2016 performance of membrane distillation].

To date, two common types of DCMD membrane configurations are in use, namely hollow fibre or tubular, wherein the membrane is normally made from PP, PVDF, and PVDF-PTFE composite material, and flat sheet or plate, where the membrane is normally made from PP, PTFE, and PVDF (Camacho et al., 2013). The flat sheet configuration has a much smaller contact area than the tubular configuration, but it is a lot easier to construct and clean, and consequently easier to perform experiments on.

Research by Eyekens (2015) indicated that commercial PE, PVDF and PP membranes showed higher retention of salt on the membrane interface, whilst on the scale up, pilot experiments revealed that the retention of salt was lower by 1-2%. The lower retention of salt was best explained by the fact that there were small defects in the membrane, which were difficult to prevent in thin electrospun membranes. These defects create a passage between the two compartments that lowers the salt retention due to salt flux due through the defect.

One of the key properties is the thermal conductivity of the membrane. The thermal conductivity of the membrane must be as low as possible to reduce the heat loss due to the conduction in the membrane wall as presented in the equation:

$$Q_c = \frac{k_m}{d} (T_{f,m} - T_{p,m}) \quad (10)$$

Where Q_c is the heat loss through conduction, d is the membrane thickness, $T_{f,m}$ and $T_{p,m}$ are the feed and permeate temperatures respectively and k_m is the thermal conductivity of the membrane, which is a property of the structure, porosity, and the intrinsic thermal conductivity of the polymer.

Furthermore, a membrane with a higher mechanical and chemical stability to withstand the feed solution would show better performance.

Table 1 shows the different thermal conductivities of the different membranes that are applicable on a commercial basis:

Table 1: Experimentally determined membrane properties

Polymer	Density	Surface energy ($\times 10^{-3} \text{N.m}^{-1}$)	Thermal conductivity at 25°C ($\text{W.m}^{-1}.\text{K}^{-1}$)	Thermal conductivity at 75°C ($\text{W.m}^{-1}.\text{K}^{-1}$)	Melting point (T_m)	Contact angle
PTFE	2.16	19.1	0.25-0.27	0.29	342	135
PVDF	1.78	30.3	0.17-0.19	0.21	165-172	130
PP	0.91-0.93	30	0.11-0.16	0.20	160-175	141
PE	0.92-0.96	33.2	0.1-0.6	0.3-0.5	96-137	120
PES	1.37	1.37	0.145	0.16	340-390	140

Material effects on the LEP were evaluated based on the contact angles of the materials based on the values that were found in literature review:

From Table 1, the effect of the contact angle on the hydrophobicity of the polymer is very significant. Stretched PTFE membranes generally have contact angles of 133-139°. PP has a high contact angle of 141°. Since this polymer has a lower surface energy in comparison to PTFE, it suggests that besides the intrinsic hydrophobicity of a material, other factors also influence the final contact angle. It is a well-known fact in surface engineering that an increased surface roughness increases the final contact angle (Lafuma, 2003). In addition, PE, untreated PVDF and electrospun PVDF all have a lower contact angle of around 120°. PES is not intrinsically hydrophobic and hence, an additional treatment is required for all PES membranes.

2.5.2 Wetting resistance or Liquid Entering Pressure (LEP)

The wetting resistance or Liquid Entering Pressure (LEP) is the minimum pressure required to wet the membrane and is a significant membrane characteristic. The LEP depends on the maximum pore size and the membrane hydrophobicity. It is directly related to feed concentration and the presence of organic solutes, which usually reduce the LEP. The LEP is dependent on both the membrane characteristics and on feed composition and can be estimated by Equation 11 (Dow et al., 2008):

$$LEP = \frac{-2b - B\gamma_L \cos\theta}{r_{max}} \quad (11)$$

Where P_f and P_p are the hydraulic pressure on the feed and permeate side, γ_L is the liquid surface tension, θ is the liquid-solid contact angle (liquid surface tension), r_{max} is the maximum pore radius, and B is a geometric pore coefficient determined by pore structure (equal to 1 for cylindrical pores). Zianhua et al. (2010) studied the impact of salt concentration (NaCl) on the water surface tension and found the following relationship:

$$\gamma_{new} = \gamma_i + 1.467c_f \quad (12)$$

Where γ_i is the surface tension of pure water at 25°C (72 mN/m). As a result, membranes that have a high contact angle (high hydrophobicity), small pore size; low surface energy and high surface tension for the feed solution possess a high LEP value (Alklaibi & Lior, 2005).

The effect of pore size on LEP is clearer when a solution of low surface tension is processed. In order to avoid wetting of membrane pores, the pore size must be as small as possible, which contradicts the requirement of higher MD permeability. Alkhudhiri et al. (2012) suggested that the maximum pore size to prevent wetting should be between 0.1-0.6 μm .

Typical LEPs are reported for values of about 5.5 bar. Table 2 reports typical values for surface energies for some polymeric materials.

Table 2: Typical commercial flat sheet membranes commonly used in MD (Khayet, n.d.)

Trade name	Manufacturer	Material	Mean pore size (μm)	LEP _w (kPa)
TF200	Gelman	PTFE/PP	0.20	282
TF450	Gelman	PTFE/PP	0.45	138
TF1000	Gelman	PTFE/PP	1.00	48
GVHP	Millipore	PVDF	0.22	204
HVHP	Millipore	PVDF	0.45	280
FGLP	Millipore	PTFE/PE	0.20	124
Gore	Millipore	PTFE	0.20	368
Gore	Millipore	PTFE	0.45	288
Gore	Millipore	PRFE/PP	0.20	463

2.5.3 Membrane thickness

(i) Membrane thickness effect on thermal efficiency

Most of the commercially available membranes that are used in MD have thicknesses ranging from 20-200 μm (Wu, 2014). In some cases, the membranes have thicknesses that are up to 300 μm , although these membranes and their use is not common. Smolders and Franksen (1989) stated that the thickness of the membrane gives important information on both the mechanical strength of the membrane and the fluxes to be expected.

While studies regarding DCMD considered the optimal membrane properties for seawater desalination few studies have focused on the optimal membrane properties in the high concentration regime; mainly aiming at optimizing the membrane thickness (Field et al., 2013; Ali et al., 2012; Rao et al., 2014; Essalhi, 2013). In a review published by Curcio and Drioli (2015) it was stated that the literature still lacks clear and conclusive statements concerning the thickness effect (Drioli et al., 2015).

Studies by Adnan et al. (2012) noted that there is an inversely proportional relationship between the membrane thickness and the permeate flux. The permeate flux is reduced as the membrane becomes thicker, because the mass transfer resistance increases, while heat loss is also reduced as the membrane thickness increases. A theoretical study was conducted by Lagana et al. (2001) to relate the effect of membrane thickness to the flux or model equations. The conclusion drawn from this study was that the optimum membrane thickness lies between 30-60 μm . Literature addressing membrane thickness is presented in Table 3.

Table 3: Membrane thickness from various membrane polymers used

Author	Membrane Type	Remarks	NaCl concentration (wt.%)	Feed Conditions
(Gostoli & Sarti, 1987)	PTFE (60 μm) PTFE + air gap (1 cm)	Flux of thin membranes is more affected by salinity	0.3	$T_m = 50^\circ\text{C}$ $\Delta T = 5-30^\circ\text{C}$ $V = 0.35 \text{ m/s}$
(Lagana, Barbieri, & Drioli, 2000)	PP (120 μm)	Optimal thickness (30-60 μm)	-	-
(Martinez, 2003)	GVHP (100 μm)	Optimal thickness depending of concentration (10-60 μm)	0-20	$T_f = 40^\circ\text{C}$ $T_p = 20^\circ\text{C}$ $V = 0.35 \text{ m/s}$
(Wu, Wang, & Field, 2014)	Electrospun PVDF	Optimal δ depending on heat transfer in the channels, feed temperature and membrane permeability (10-20 μm)	0-9	$T_f = 45-65^\circ\text{C}$ $T = 20^\circ\text{C}$
Wu [20]	Electrospun PVDF (27-58 μm)	Optimal δ depending on heat transfer in the channels, feed temperature and membrane permeability (10-20 μm)	0-9	$T_f = 45-65^\circ\text{C}$ $T_p = 20^\circ\text{C}$ $v = \text{not specified}$
Martinez [18]	GVHP (100 μm), TF200 (60 μm)	Asymptotic value for larger δ , sharp decline of energy efficiency at low δ especially at higher concentrations	0-20	$T_f = 40^\circ\text{C}$ $T_p = 20^\circ\text{C}$ $v = 0.35 \text{ m/s}$
Essalhi [21]	Electrospun PVDF (144-1529 μm)	Asymptotic value for larger δ , decline of energy efficiency at low δ , especially at higher concentrations	0-6	$T_f = 40-80^\circ\text{C}$ $T_p = 20^\circ\text{C}$ $v = \text{not specified}$

Martinez (2008) also found that at low membrane thickness, there was a sharp drop in the energy efficiency, which was consistent with findings in other bodies of literature.

The membrane thickness is a significant parameter in the determination of the resistance to mass transfer. Thus, to achieve a high permeability on the membrane, the membrane should be as thin as possible. On the other hand, better thermal efficiency can be affected when the membrane is as thick as possible; this is because, in membrane distillation, heat loss by conduction takes place through the membrane matrix (Lawson, 1997; Schofield, 1987)

It is generally accepted that the permeability is enhanced by reduction in the membrane thickness, by increasing the porosity and pore size.

(i) Membrane thickness effect on salinity

Previous studies have also been carried out on the interactions of the membrane thickness and the salinity of the brine solutions. Some studies have confirmed that for low salinities, thin membranes are more suitable (Lagana, 2000; Essalhi, 2013). Also other studies have indicated that at thicker membrane structures the membranes perform better at higher salinities.

Salinity plays an important part in the determination of optimal membrane thickness. Studies by Gostoli et al. (1987) indicated that for thin membranes the flux is more affected by concentration. The presence of salt reduces the water vapour partial pressure in the feed. With decreasing membrane thickness, the effect of salinity becomes more pronounced. At a certain thickness, the reduction of the driving force due to temperature polarization and salts counterbalances the increased permeability, resulting in an optimum membrane thickness for flux. Moreover, thinner membranes are more sensitive to salinity compared to thicker membranes (Eyekens et al., 2016). In a study by Martinez and Rodriguez-Maroto, the transmembrane flux for MD using supported PVDF and PTFE membrane (Martinez and Maroto, 2008) concluded that thicker membranes had higher flux in high salt concentration due to decreased temperature polarisation across the membrane. Thus with increasing salinity, both flux and energy efficiency of the thin membranes are severely reduced, especially at low temperature differences and flow velocities. At high salinities, thin membranes can only be used if sufficient driving force is provided.

2.5.4 Membrane pore size and pore distribution

Several investigations have focused on a few membranes with most likely variation in membrane pore size (Pataranawick, 2003; Woods, 2011). Membranes with pore size between 100 nm to 1 μm are usually used in MD systems, upon which the permeate flux increases with increasing membrane pore size (El-Bourawi et al., 2006). El-Bourawi et al. (2006) emphasized that the mechanism of mass transfer can be determined based on the membrane pore size and the mean free path through the membrane pores taken by transferred molecules (water vapour). A large pore size is required for high permeate flux, while the pore size should be small enough to avoid liquid penetration.

Several authors have reported that it would be worthwhile to use mean pore size to determine the vapour transfer coefficient instead of pore size distribution (Phattaranawik & Jiratananon, 2003; Martinez, 2003; Imdakm & Matsuura, 2005; Khayet, n.d.; Khayet, n.d.). This was also confirmed by Martinez (2003) who

obtained a reasonable vapour transfer coefficient when the mean pore size and pore size distribution were used.

2.5.5 Membrane porosity

Membrane porosity refers to the void volume fraction of the membrane (defined as the volume of the pores divided by the total volume of the membrane).

The porosity (ε) can be determined by the Smolder-Franken equation (Khayet & Matsuura, 2001).

$$\varepsilon = 1 - \frac{\rho_m}{\rho_{pol}} \quad (13)$$

Where ρ_m and ρ_{pol} are the densities of membrane and polymer material, respectively.

Studies by Zhang et al. (2012) and Zhang (2010) confirmed that membrane porosity contributes greatly to the flux, temperature polarisation and thermal efficiency. The high porosity was favourable for high flux, low temperature polarisation coefficient (θ) and high thermal efficiency. According to El-Bourawi et al. (2006), membrane porosity in the MD system varies between 30 to 85%.

2.5.6 Tortuosity

Tortuosity (τ) is the deviation of the pore structure from the cylindrical shape. As a result, the higher the tortuosity value, the lower the permeate flux. A correlation was suggested by Surapit et al. (2006):

$$\tau = \frac{(2 - \varepsilon)^2}{\varepsilon} \quad (14)$$

A lower tortuosity and higher porosity both increase the membrane permeability and therefore result in a higher flux for all membrane thicknesses. The energy efficiency is improved for lower tortuosity, higher porosity and lower membrane thermal conductivity. In these cases, the flux is improved, while heat loss due to conduction is not affected (in the case of tortuosity) or even reduced (in the case of porosity and thermal conductivity).

2.5.7 Backing structures

Commercial membranes used in MD have low thicknesses normally not more than 200 μm . Thus, thinner membranes less than 60 μm are prone to damage due to low mechanical stability, and hence mechanical defects. A way to remedy that is by the use of supporting material consisting of nylon or scrim supports (Adnan, 2012). In other instances, hydrophobic polymers such as PE or PP are also used for this purpose. However, as the pore size of these nonwoven supports is above 1 μm the support material is considered to be wetted during the MD operation. Whilst the supported material adds mechanical strength to the membrane, it also imposes an additional resistance in the process. The role of backing layers has not yet been investigated quantitatively at a larger scale. However, it was noted that backing layers have an effect on membrane structure especially on the thermodynamic phenomenology (Winter et al., 2013). The addition of support material reduced the flux across the membrane. It was understood

that a complex network of thermal resistances is formed by the presence of a backing material, the material itself forming an additional resistance to the heat transfer. In addition to that, the cross sectional area for diffusion might also be imparted by the presence and the absence of the backing layers. This results in the additional mass transfer resistance (Mastuura, 2005)

In their study, Adan and co-workers (Adan et al., 2012) pointed out that non-supported membranes had better performance than supported membranes due to the absence of flux blockage at the permeate side and additional temperature polarisation by the membrane support material. However, their findings could not be very conclusive of the effect, as their study was limited only to PTFE membranes.

To date, few systematic studies have been performed on the optimal properties of the hydrophobic layer in supported composite membranes (Martinez et al., 2008). According to Qtaishat et al. (2009), the influence of the hydrophobic material thermal conductivity can be neglected.

The properties of the support layer also affect the membrane distillation performance and can be adjusted to increase the membrane performance by (Qtaishat et al., 2009; Su, 2010):

- Reduction of the support thickness to reduce the temperature polarization and increasing the flux
- Increased thermal conductivity results in more heat transfer through the wetted support, less temperature polarization, and a higher driving force and flux through the hydrophobic membrane layer.

2.5.8 Mechanical Strength

Membranes exhibit a degree of deformation before fracture. These are evaluated in terms of the stress and strain before fracture (Raab et al., 2001). Table 4 illustrates the different stress and strain with the corresponding Young modulus values for different membrane types (Eyekens et al., 2016):

Table 4: Young modulus for different membrane types

Membrane	Strain at break (%)	Stress at break (MPa)	Young's modulus (MPa)
PE	21	19.3	81
PES	20	16.5	549
PP	70	1.2	19
PTFE	192	13.2	8
PVDF	19	5.7	156

Systematic tests by Eyekens et al. (2016) showed that unsupported PP and PTFE membranes needed little stress to deform, thus displaying more strain at breakage and bending. On the other hand, PVDF has a lower strain at breaking, thus requiring much more stress to break the membrane.

2.5.9 Cost of production of membranes

The most commonly used membranes in MD include the stretched PTFE and PE membranes and the phase inverted PVDF and PP membranes. The cost of the membrane depends on several factors, most

prominently the method of production. Literature survey has pointed out that PTFE membranes are mainly produced by stretching process, which makes the membrane material much more expensive (Eyekens, 2016). In addition, the authors argued that the production of thicker membranes is equally costly. On the other hand, commercially useable PP, PVDF and surface modified PES membranes are produced by isotropic phase inversion. However, literature still lacks clear and conclusive statements on the cost of the membranes.

3 MDC Experimental Set Up and Methodology

Details regarding the use of equipment and materials, as well as experimental procedures followed during all experimental runs conducted are provided in this chapter along with descriptions of the equipment and instruments used.

All experiments were conducted at the Cape Peninsula University of Technology, Bellville, Chemical Engineering and Chemistry Building.

3.1 Experiment set-up

The Direct Contact Membrane Distillation (DCMD) experimental set up used in the preceding WRC Project K5/2223//3 was used for this project.

In the configuration of a typical DCMD, the membrane is in direct contact with the liquid phases and is best suited for desalination and concentration of aqueous solutions. DCMD is characterised by an increased flux when compared to other configurations such as Air Gap Membrane Distillation (AGMD), Vacuum Membrane Distillation (VMD) and Sweep Gas Membrane Distillation (SGMD).

The MDC setup as described by Khayet (n.d.) and Tun et al., 2005 was adopted such that the working volume for the crystalliser was 4 L for this study. The general configuration of the DCMD experimental set up used is shown in Figure 4 and the basic design of the membrane element cell that was used is shown in Figure 5.

A list of the key equipment components and their specific function is provided in Table 5.

The circulation pumps used in the MD process are two peristaltic type Watson & Marlow pumps. Peristaltic pumps were selected for the following advantages:

- The pumping mechanism is never in direct contact with the pumped fluid and the tubing (wear parts) in the pump head is easily interchangeable.
- The adjustable variable speed of the peristaltic pumps allows for a broad flow rate set point range with precision flow rates.
- If required, the pump is able to communicate to a desktop computer via RS 232 to the USB port.

The feed solution was heated using a thermostatic circulating unit (Lauda RE415). The heating solution (Kryo 40) was circulated through a jacketed feed water tank. The heated solution was pumped through the outer cavity "Jacket" of the tank. The conductive heat transfer between the jacket and the inner fluid volume heats up the primary solution without direct contact to avoid any contamination, the boundary between the primary and secondary solution was made from stainless steel 304.

A Chiller (Lauda RP855) was installed on the permeate side to cool down the permeate stream and create the necessary vapour pressure difference between the heated and the cooled down solution. The solution on the product circuit is indirectly cooled by means of a copper tube heat exchanger placed into the product water tank. The heat exchanger design is based on the specific heat transfer coefficient of the copper tubing and the heat removal required based on an energy balance over the membrane distillation system.

Agitators were installed in the tank to promote effective homogeneous mixing and optimise heat transfer. The overhead agitator has a variable speed drive (VSD) with the potential for measuring output power, from this, the torque increase could be calculated and ultimately a calculation could be done to measure the change in viscosity.

Electrical conductivity was used as a proxy for the TDS. Although, not completely as accurate as the laboratory TDS analysis, it is usually very close to the actual TDS value if a meaningful correction factor is applied. Conductivity cells were placed in the feed tank, product tank as well as before and after the MD unit. The conductivity cells were also connected to the analogue inputs in the same manner. Similarly, they were scaled to the required range.

pH probes were installed into the feed and product tanks. The pH probes provided a 4-20 mA output converted by the programmable logic controller (PLC) into a reading. The pH probes were not directly connected to a PLC input, in reality, they are connected to a pH controller that converts the millivolt output signal into readable data for the PLC unit.

The PLC controller actively monitored all signals, which in turn plotted them into graphs for easy visualisation. This data was displayed on the human-machine interface (HMI). The control of the process was also executed on this unit. Memory shortage on the PLC forced the data to be automatically exported onto a desktop PC or SD card to capture the data for the entire duration of the experiment.

Table 5: Direct Contact Membrane Distillation set up key equipment components and their specific function

Equipment Description	Purpose
Membrane distillation unit	To concentrate the stream by producing pure water
Jumo Conductivity meters	Measures the conductivities and temperatures of the feed and product
Thermo Scientific Chiller x 2	Maintains solution temperature at predetermined level
Watson Marlow 620S/R Peristaltic pumps x 2	Necessary to pump solution to and from the crystalliser & membrane unit
4 L Jacketed crystalliser x 2	To crystallise out salts from solution
Overhead agitator with variable speed drive x 2	Provides adequate mixing of the solution
Equipment frame	Needed to house equipment
Programmable Logic Controller (PLC) system	To record all the relevant data in real time (Temperature, pressure, conductivity, etc.)
Auxiliary equipment (piping, valves, tubing, insulation, clamps, etc.)	

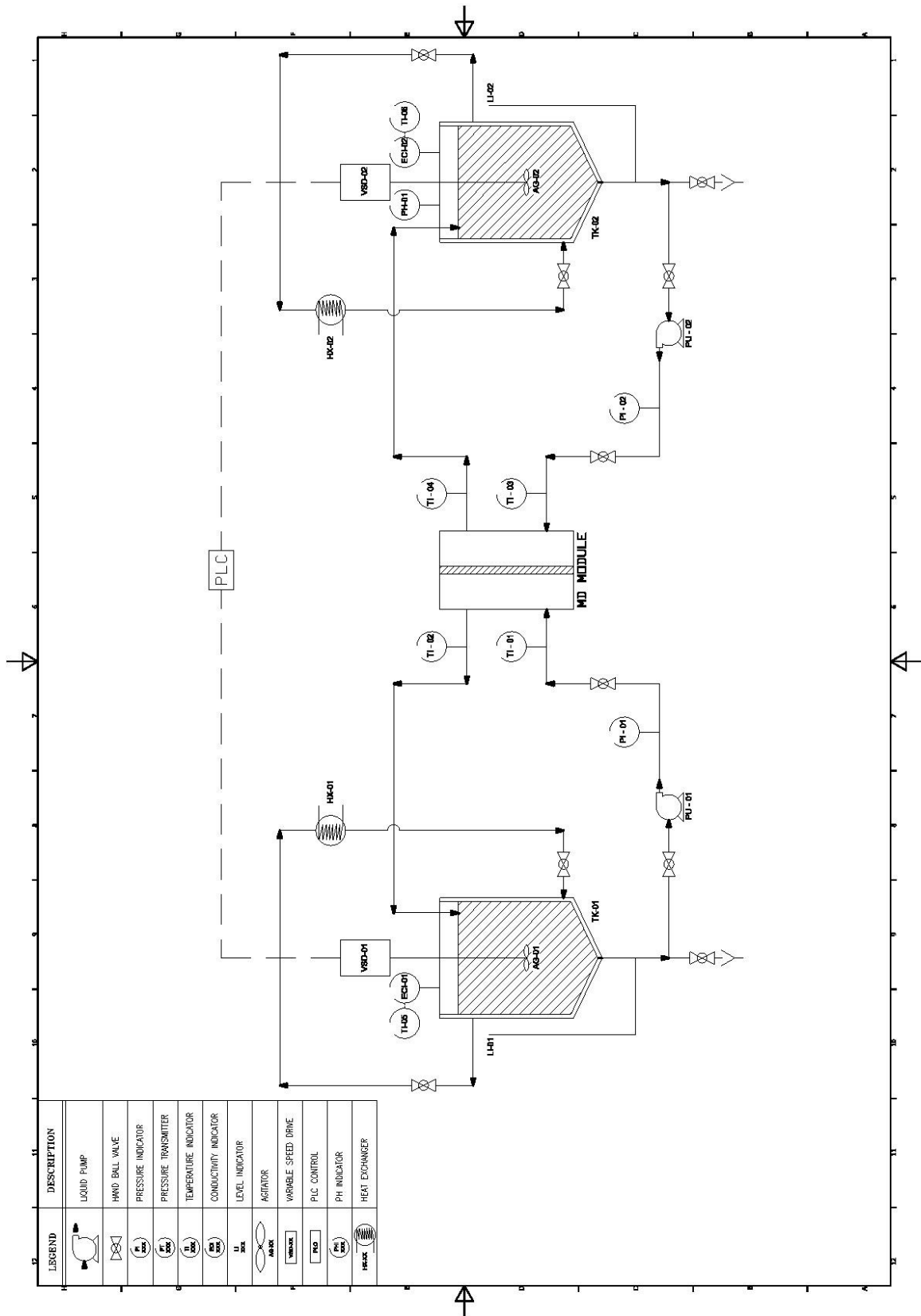


Figure 4: General configuration of the DCMD experimental set up

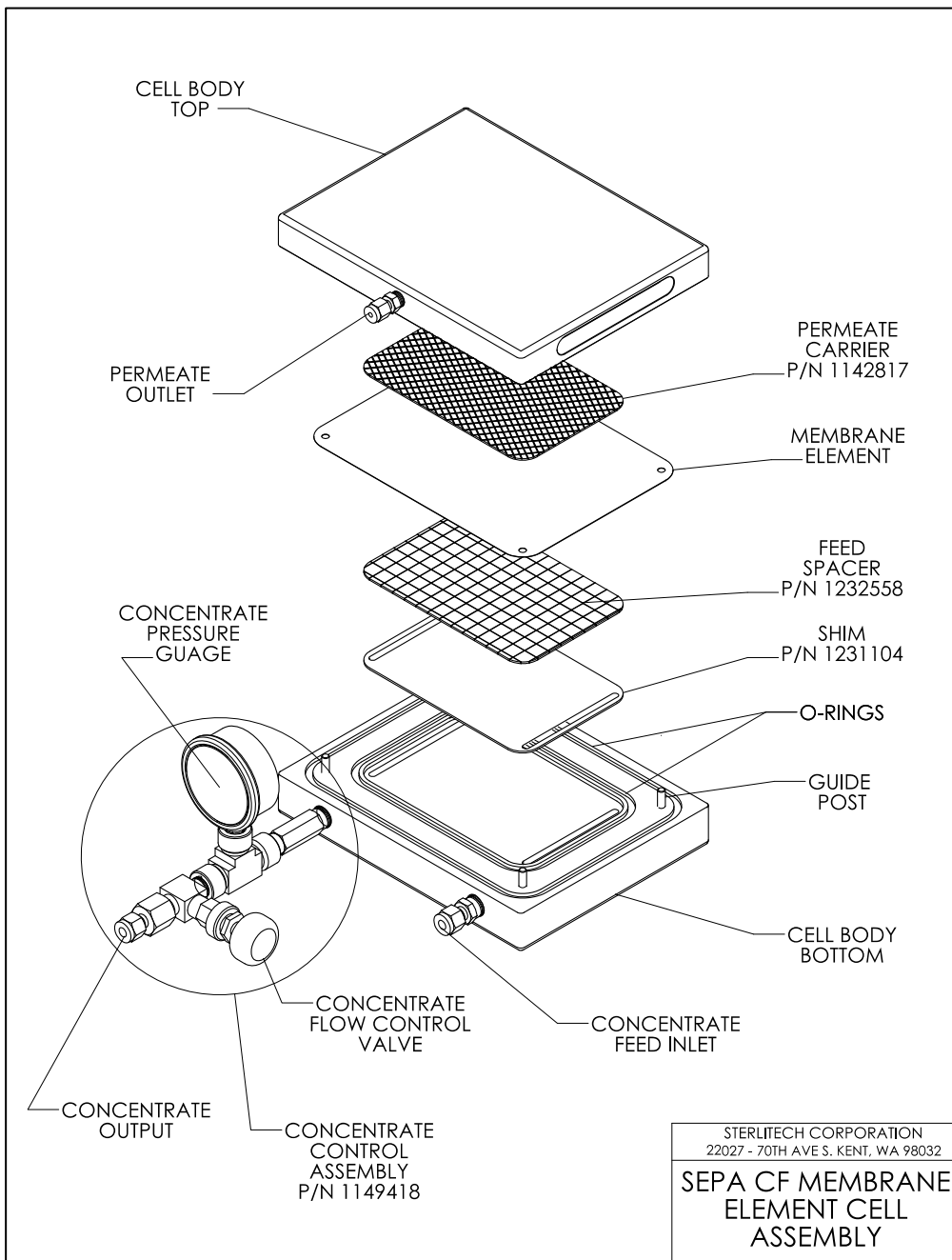


Figure 5: Membrane element cell assembly of the DCMD experimental set up



Figure 6: Photograph of commissioned DCMD experimental set up



Figure 7: Photograph of commissioned DCMD experimental set up

3.2 Experimental Methodology

The following parameters needed to be measured and recorded accurately, to study the membranes actual performance:

- I. The temperature in the feed solution, permeate solution, and the transmembrane temperature difference are precisely measured.
- II. Conductivity, measured in the feed and the permeate solution in order to verify the membranes salt rejection and the formation of crystals in the feed solution.
- III. Flow rate is controlled at the feed and permeate side in order to set the permeate flux rate.
- IV. A balance will be used to calculate the permeate flux rate.
- V. pH measurement in the feed solution to ensure acceptable feed water quality.

3.2.1 DCMD equipment testing methodology

The experiments were conducted in batch-mode whereby the feed (salt solution) ran co-current to the product (deionised water) with the membrane module separating the two streams. These two systems, i.e. the feed stream and the product stream, were driven by two separate peristaltic pumps (Watson & Marlow).

These pumps were calibrated for the specific tubing used in this experiment, so that the volumetric flow rate could be determined for each experiment¹. The pressure exiting the pumps was monitored to ensure that there were no blockages in the line.

Both the feed and product storage tanks had a liquid holding capacity of ~4 litres.

The feed solution was heated using a thermostatic circulating unit (Lauda RE415). The heating solution (ethylene glycol solution/Kryo 40) was circulated through a jacketed feed water tank. The heated solution was pumped through the outer cavity "Jacket" of the tank. The conductive heat transfer between the jacket and the inner fluid volume heats up the primary solution without direct contact to avoid any contamination. The boundary between the primary and secondary solution was made from stainless steel 304.

A Chiller (Lauda RP855) was used on the permeate side to cool down the permeate stream and create the necessary vapour pressure difference between the heated and the cooled down solution. The solution on the product circuit is indirectly cooled by means of a copper tube heat exchanger placed into the product water tank. The heat exchanger design is based on the specific heat transfer coefficient of the copper tubing and the heat removal required based on an energy balance over the membrane distillation system.

Agitators were installed in the tank to promote effective homogeneous mixing and optimise heat transfer. The overhead agitator has a variable speed drive (VSD) with the capability of measuring output power from this and consequently the increase in torque increase and the relative change in viscosity.

To measure the temperature, PT 100 temperature transmitters were used for the recording of the temperatures at the specified locations in the MD setup. The temperature transmitters were connected to the analogue input modules of the PLC. The transmitters transmit a 4-20 mA output, which is converted by the PLC into degrees Celsius or any other unit of measure. The 4mA is scaled to the minimum measurement required in the setup and likewise the 20 mA corresponding to the maximum temperature within the system. The placement of the PT 100 transmitters was carefully selected within the setup to minimise the length of the signal cables to allow for more accurate readings.

Electrical conductivity was used as a measurement of the feed and product streams and to determine their calculated total dissolved solids (TDS) concentration. Conductivity probes were placed in the feed tank, product tank as well as before and after the MD unit. The conductivity probes were also connected to the analogue inputs in the same manner and scaled to the required range.

pH probes were installed in the feed and product tanks. The pH probes provided a 4-20 mA output converted by the PLC into a reading. The pH probes were not directly connected to a PLC input, in

¹ The pumps were calibrated as per the pump manual. These values are then stored in the pump.

reality, they are connected to a pH controller that converts the millivolt output signal into readable data for the PLC unit.

3.2.2 Measurement of experimental variables and data logging methodology

A PLC system measured the temperature into and out of the feed and product sides of the membrane module. The conductivity in each tank, the pH of the product tank and the pressure after each pump was also recorded. The data logging system was configured to measure and log measurements every 15 seconds.

The agitator speed was controlled via the PLC and inputs for the given flow rates and heat exchanger temperatures were also manually inputted to record most of the key parameters that influence the system. The tank level was measured and recorded manually. The key parameters that were recorded included the volume change, electrical conductivity, temperatures and flow rates. The volume change was used to determine the volumetric flux across the membrane by using Equation 15.

$$Flux = \frac{Volume\ of\ water\ extracted\ (ml)}{Membrane\ area\ (m^2) \times Timeperiod\ (h)} \quad (15)$$

3.2.3 Experimental procedure

The feed and product temperatures were set to the required temperature at the entrance to the membrane module from both the feed and product side. These had to be controlled indirectly by adjusting the heat exchanger temperatures.

Before switching on the experimental apparatus, the valves to the membrane module were closed for both the feed and product side. Four litres of the sample solution were prepared and poured into the feed tank. The conductivity probe was submerged into the solution. The product tank was then filled with sufficient deionised water for the conductivity probe to be submerged.

Before switching on the experimental apparatus, the valves to the membrane module were closed for both the feed and product side. Four litres of the sample solution with the composition required to make up the feed solution was prepared and poured into the feed tank. The conductivity probe was submerged into the solution. The product tank was then filled with sufficient deionised water for the conductivity probe to be submerged.

The circulating temperature control systems for each side of the membrane module, i.e. feed and permeate side were then switched on and set to the required temperatures. The pump speed was set to the maximum pump flow of 25 L/min to achieve the highest heat transfer rate.

The membrane was installed into the module with two rubber gaskets/O-rings to keep the membrane in place and to seal the system.

When the tanks had reached the required operating temperatures, the valves to the membrane module were opened and the pumps switched on. The system was given sufficient time to stabilise before data logging was initiated as the temperature of the circulating lines and membrane module had to reach the required temperature. During this time the inlet temperature for both the feed (T_1) and product (T_3) side into the membrane module were monitored to ensure that they were at the required temperatures for the specific runs. The heat exchanger temperatures were adjusted accordingly if T_1 and T_3 were not at the required level.

The tank level readings were recorded at 10-minute intervals for the first 180-minute of a run and subsequently 30 minutes or 1-hour intervals for runs extending beyond 180-minutes in duration.

This was done by stopping the pumps for 10 seconds, recording the level and switching the pumps on again. For instances where the level readings could not be obtained at a specific sampling time for whatever reason during any of the experimental runs, these were omitted from the average flux calculated for each experimental run and marked with a dash symbol in the raw data.

All experiments had a duration of 3 hours except for the effect of fouling experiments which were conducted on the Type 1 and Type 2 brine. These experiments were run for a longer duration as stated in the 6.1.1 Scaling/fouling effects on MD performance for prepared Type 1 brine

3.3 Selection of model brines for the study

Two characteristically distinct brines with varying dominant ion valences and scaling propensities (referred to as Type 1 and Type 2) were investigated. A description of the characteristics of Type 1 and Type 2 brines is provided below:

Type 1 Brine

Type 1 brine was a monovalent ion dominant, sodium chloride hypersaline solution with little to no scaling or fouling propensity within the range of water recoveries anticipated using membrane distillation.

Table 6: Composition of synthetic Type 1 brine NaCl concentration levels used in this study

Chemicals	Molecular weight (g/mol)	Concentration (mg/L)		
		35 000	50 000	65 000
Sodium Chloride (NaCl)	58,44	35 000	50 000	65 000

Type 2 Brine

Type 2 brine contained a combination of monovalent and divalent ionic species. As a result of the presence of calcium, magnesium, sulphate and bicarbonate ions, Type 2 brine had a propensity towards scaling/fouling within the range of water recoveries anticipated using membrane distillation.

Both synthetic and real brine solutions that fell within the classification of Type 2 brine were investigated in this study. The synthetic brine was used to simulate real brine sample generated from brackish water reverse osmosis (RO) processes associated with industrial and/or coal mining applications.

The composition of the synthetic Type 2 brine investigated in this study is shown in Table 7:

Table 7: Chemical make-up of synthetic coal mine brine

Chemicals	Molecular weight (g/mol)	Concentration (mg/L)	Feed TDS (mg/L)
Sodium Bicarbonate (NaHCO ₃)	84	957	11870
Sodium Sulphate (Na ₂ SO ₄)	142	6778	
Sulphuric Acid (H ₂ SO ₄)	98	1293	
Magnesium Chloride (MgCl ₂)	95	1770	
Calcium Hydroxide (Ca(OH) ₂)	74	977	

The synthetic Type 2 brine above was based on a real coal mining effluent that was treated with an RO process. The resultant TDS of this RO brine was 11870 mg/L and was used as the lower TDS option of the two variants of Types 2 brines investigated in this study.

The second variant of Type 2 brine investigated was a higher TDS variant that was modelled on the second stage RO process brine after the first stage had undergone interstage de-supersaturation. The feed water analysis to the second stage RO post desupersaturation was calculated based on the aqueous thermodynamic equilibrium at the selected desupersaturation pH using OLI Stream Analyser version 10. The composition of the higher TDS (27025 mg/L) variant Type 2 brine investigated in this study is shown in Table 8.

Table 8: Chemical make-up of the desupersaturated synthetic coal mine brine that was treated with RO (stage two RO)

Chemicals	Molecular weight (g/mol)	Concentration (mg/L)	Feed TDS (mg/L)
Sodium Bicarbonate (NaHCO ₃)	84	1611	27025
Sodium Sulphate (Na ₂ SO ₄)	142	17839	
Sulphuric Acid (H ₂ SO ₄)	98	834	
Magnesium Chloride (MgCl ₂)	95	3772	
Calcium Chloride (CaCl ₂)	111	2969	

3.4 Selection of key membrane characteristics to be investigated

The selection criteria for the key membrane characteristics investigated for this study was based on the information described in the literature review in 0. This information identified the most important membrane characteristics to be investigated as well as the typical ranges of the various parameters to consider. A summary of the key findings can be seen below:

3.4.1 Hydrophobicity

Hydrophobic membranes that were initially developed for microfiltration applications are typically used in most commercial MD system applications. Many of the polymer materials used such as PVDF, PP, PTFE, PE and PES have great wetting resistance due to the low surface tension on the surfaces. All of these polymers yield high contact angle within the range of 120-140° which is very significant in terms of the required hydrophobicity. Most of the membranes used currently demonstrated extremely good hydrophobicity.

For this study, PVDF membranes within the contact angle range stipulated above were selected as they are the widely used and have demonstrated excellent hydrophobic tendencies in previous studies from a range of researchers.

3.4.2 Membrane Thickness

Many of the commercially available membranes that are used in MD have thickness ranging from 20-200 µm. An inverse relationship was identified between membrane thickness and permeate flux. The membrane thickness gives important information on both the mechanical strength and the fluxes to be expected. It is generally accepted that the permeability is enhanced by reduction in the membrane thickness, by increasing the porosity and pore size.

For this study, a membrane thickness ranging between 100-150 µm was selected owing to the fact this range provides the best compromise between flux and mechanical strength and is by and large the thickness range used in most commercially available membranes for this exact reason.

3.4.3 Membrane Porosity

Membrane porosity has an influence on flux, temperature polarisation and thermal efficiency. Whilst high porosities are advantageous in term of promoting high fluxes, low temperature polarisation coefficient (θ) and high thermal efficiencies, the downside is that the higher the porosity, the lower the mechanical integrity of the membrane. Consequently, although membrane porosities in the MD system can vary between 30 to 85%, most membrane manufactures and applications settle on a porosity not exceeding 85% as this has been found to be the optimal compromise between flux and mechanical integrity.

For the purposes of this study, membranes with a porosity of 75% were selected.

3.4.4 Membrane Pore Size

Membrane pore size between 100 nm to 1 µm are usually used in MD systems. Membrane flux increases with increasing membrane pore size. However, smaller pore sizes minimise liquid penetration. Typically, commercial flat sheet membranes commonly use a pore size range between 0.1 µm to 0.6 µm. Of all the characteristics investigated, pore size was identified to be the one with the greatest influence on MD performance as a function of feed characteristics in terms of salinity and scaling/fouling as well as transmembrane temperature differential. Consequently, pore size was selected as the key membrane characteristic variable for this study.

Due to the timing of the first wave of the Covid-19 pandemic coinciding with the procurement and importation of the commercial membranes, it proved extremely challenging to order and ship any suitable membranes due to a major supply shortage, travel and shipping restrictions as well as the restrictive import regulations during this time. Notwithstanding these challenges and the resultant 8-month delay to the project, two commercial membranes were sourced from Merck Millipore, namely the GVHP and HVHP 147mm membrane discs.

The characteristics of the GVHP and HVHP membranes are provided in Table 9 below.

Table 9: Merck Millipore GVHP and HVHP membrane characteristics

Supplier	Merck Millipore	
Membrane Name	GVHP	HVHP
Max operating temp (°C)	85	85
Pore size (µm)	0,22	0,45
Porosity (%)	75	75
Thickness (µm)	125	125
Polymer type	PVDF	PVDF

The GVHP and HVHP membranes provided a good balance between selecting membranes that are representative of those readily available on a commercial scale and being used for membrane distillation, whilst simultaneously also meeting the criteria of having a large enough differential in pore size between the two membranes which was central to achieving the objectives of this study.

4 Establishing the minimum acceptable flux for MDC and development of a flux prediction model for MDC

This chapter focusses on the methodology, results and discussions pertaining to:

1. The investigation undertaken towards determining the minimum acceptable flux below which membrane distillation as an emerging technology becomes commercially unviable relative to existing commercial brine treatment technologies
2. The development of the flux model whose utility lies in its ability to quickly ascertain whether any specific brine under consideration meets the minimum acceptable flux criterion described in Chapter 5.

4.1 Establishing the minimum acceptable flux for MDC

4.1.1 Experimental Methodology

The basic experimental methodology was as follows:

- i. From literature sources, establish the costs associated with manufacturing an MD plant and to calculate the unit cost of treatment in Rands per meter cubed (R/m^3) as a function of flux
- ii. From literature sources, establish the unit cost in Rands per meter cubed (R/m^3) of brine treatment using conventional brine treatment technologies, specifically mechanical vapour compression (MVC) and multi-effect distillation and evaporative crystallisation (MED).
- iii. Plot the cost in Rands per meter cubed (R/m^3) for MD as function of flux when compared against competing, conventional brine treatment technologies
- iv. Establish the minimum flux below which MD becomes more expensive when compared to MED or MVC would be considered commercially unviable.

4.1.2 Results and Discussion

According to Schwantes (2018), the cost of membrane distillation (MD) and mechanical vapour compression (MVC) for application in achieving ZLD is $R79,95/m^3$ and $R106,02/m^3$ respectively. Chen (2021) evaluated the cost of multi-effect distillation and evaporative crystallisation (MED) for desalinated brine treatment to be approximately $R72,47/m^3$.

The unit cost of treatment (R/m^3) using MD was calculated using a basis of 1000 m^3/day brine treatment, a membrane cost of $\$90/m^2$ as per Drioli (2006) and Noor et al. (2020) and a Rand to USD exchange rate of $R15.10$ to $USD1$. In the detailed cost evaluation for MD presented by Noor et al., (2020), the factored estimate method was used to determine the total cost of equipment. Based on this, the membrane cost to overall plant capital cost ratio was determined to be approximately 60% of the overall capital cost of the plant. Notwithstanding this, a conservative membrane cost to overall plant capital cost ratio of 20% was used for this study. This provided sufficient room for any upward variability in the cost per m^2 of

membranes, as well as the membrane cost to overall plant capital cost ratio such that the minimum acceptable flux for MDC presented was not in any way underestimated.

Figure 8 below shows how the unit cost of treatment for MD in Rand/m³ varies as function of the flux rate. The lower the flux, the greater the membrane surface area and MD modules required to achieve a particular treatment capacity.

Importantly, the graph highlights the MD flux rates below which other conventional brine treatment technologies (MVC and MED) are considered to be more cost effective than MD.

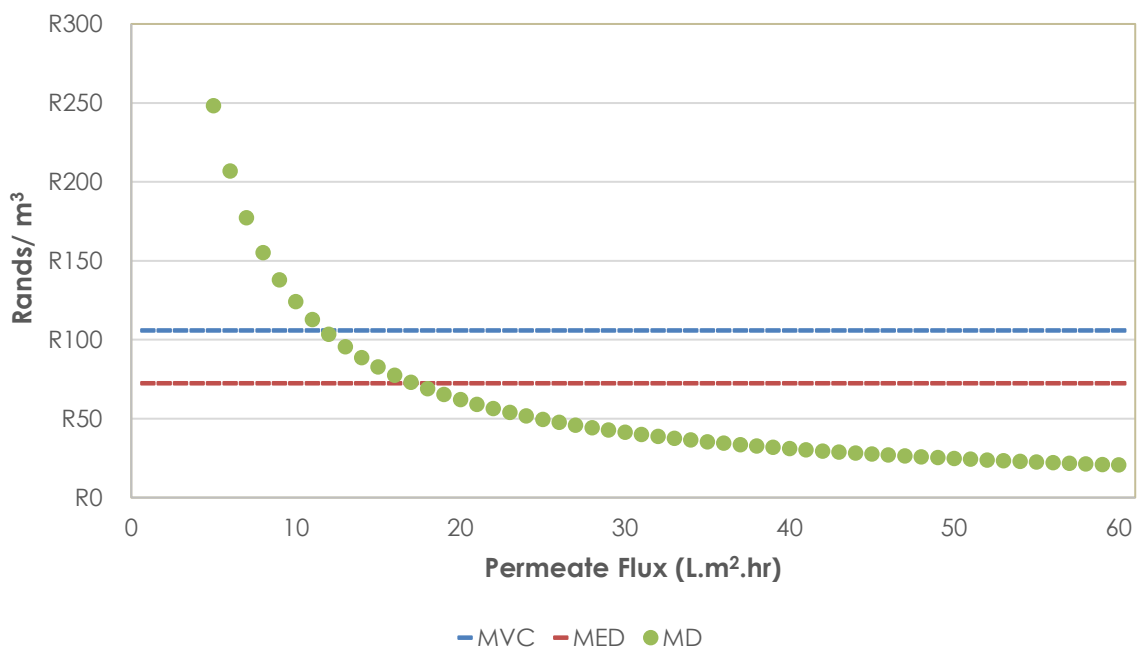


Figure 8: Cost of MD for treating highly saline brines

Based on the results shown in Figure 8 above, at fluxes below **18 L/m²·hr** for MD, other conventional brine treatment technologies such as MED and MVC appear to show better commercial viability when compared to MD.

As highlighted in the experimental results further on in this report, fluxes rates above 18 L/m²·hr are readily achieved for feed temperatures above 60°C. This is important to note as these moderate temperatures can be achieved with use of waste heat or renewable energy. As a result, the implementation of waste heat or renewable has the potential to reduce the costs by as much as 75%.

The viability of MD can potentially be significantly further enhanced by a reduction in the per unit manufacturing cost of MD membranes. This could be achieved as the economies of scale improve on the back of a broader adoption of this technology as an alternative brine treatment option.

One of the objectives of this study aimed at identifying quintessential considerations, mainly related to key membrane characteristics and performance criteria, when assessing the viability of implementing and selecting MDC over alternative technologies was the development of a flux prediction model for MDC.

4.2 Development of a flux prediction model for MDC

4.2.1 Experimental Methodology

This experiment investigated the effect that membrane pore size, increasing feed concentration and operating conditions for Type 1 Brine had on MD performance. The development of the experimental matrix and subsequent data analysis was performed using Design Expert 11 software towards developing a permeate flux model for general use with other Type 1 brines.

The range of TDS concentrations used in this experiment are provided in Table 10 along with the experimental matrix in table 11 below:

Table 10: Type 1 Brine NaCl concentration levels used

Chemicals	Molecular weight [g/mol]	Concentration [mg/L]		
Sodium Chloride (NaCl)	58,44	35 000	50 000	65 000

Table 11: Experimental matrix using response surface approach

Test #	Feed temperature [°C]	NaCl concentration [g/L]	Membrane	Pore Size [µm]
1	80	65	HVHP	0.45
2	60	35	GVHP	0.22
3	40	65	HVHP	0.45
4	40	50	GVHP	0.22
5	60	50	HVHP	0.45
6	80	35	GVHP	0.22
7	40	35	HVHP	0.45
8	60	65	GVHP	0.22
9	80	35	HVHP	0.45
10	80	50	GVHP	0.22

The process conditions for this experiment were as follows:

Brine used: Prepared Type 1 brine

Brine composition: NaCl-H₂O solution: 35 g/L, 50 g/L, 65 g/L

Temperature: T_{feed} = 40°C, 60°C, 80°C and T_{perm} = 10°C

Flowrates: F_{feed} = 130 L/hr

Run time: 3 hours

4.2.2 Results and Discussion

4.2.2.1 Effect of membrane characteristics on MD performance for Type 1 brine

Figure 9 and Figure 10 below give a 3-dimensional representation, showing the effect of a variation in feed temperature and feed concentration on the change in flux, for the treatment of Type 1 brine for the 0.22 μm and 0.45 μm membrane pore sizes respectively.

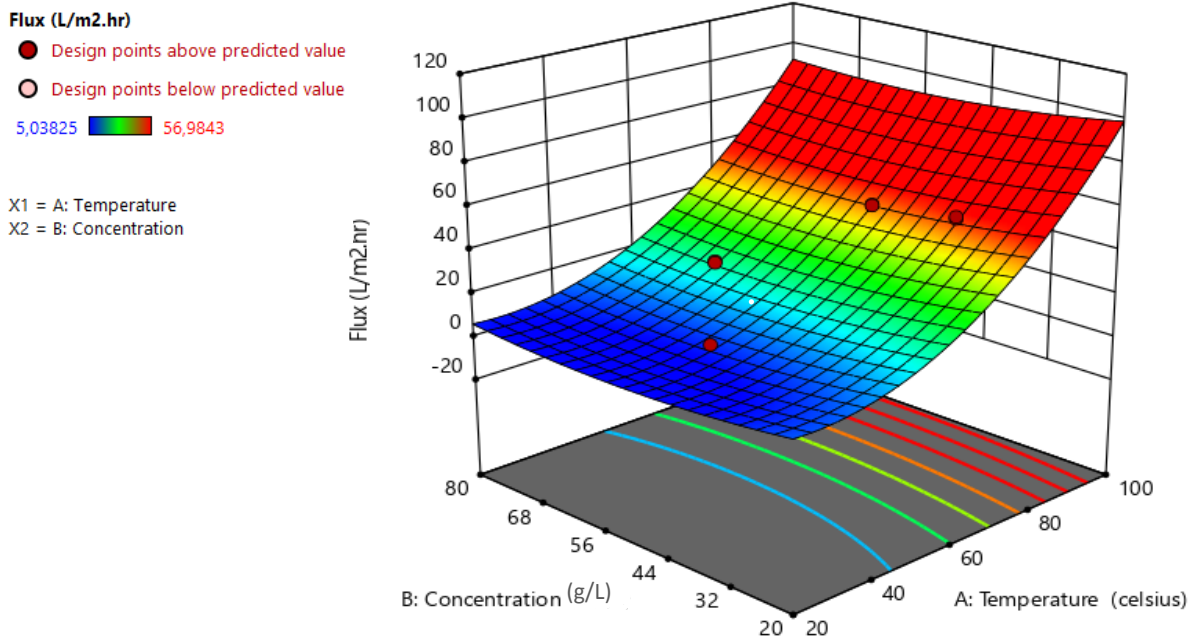


Figure 9: 3-dimensional representation of the effect of a variation in the feed temperature and feed concentration on the change in flux for Type 1 brine using the 0.22 μm membrane pore size

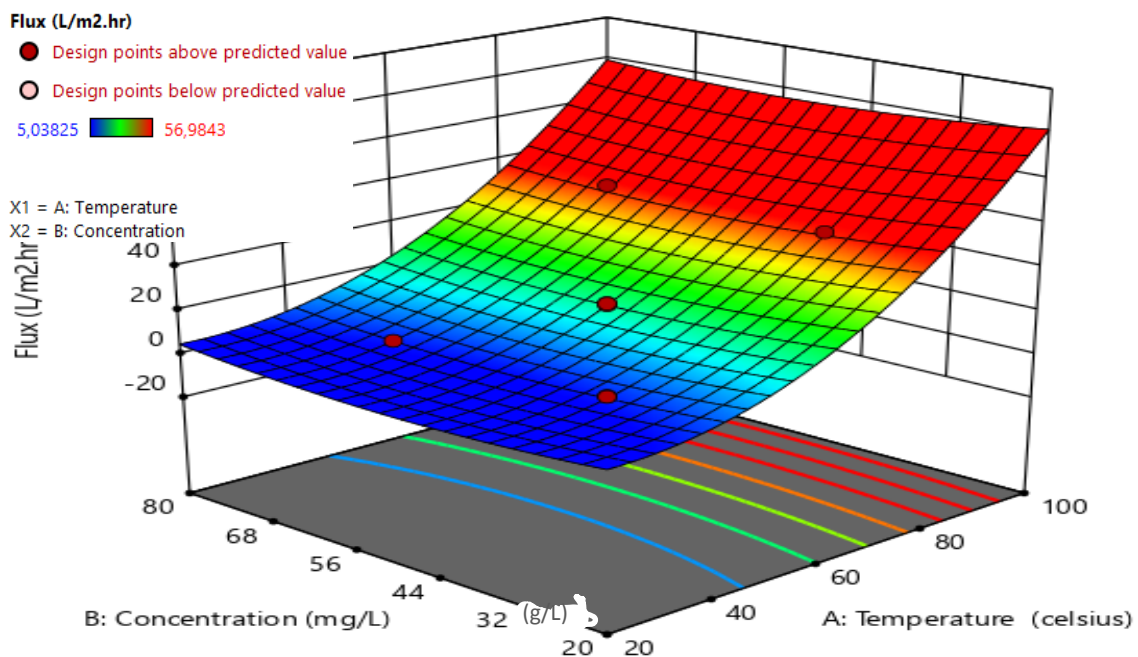


Figure 10: 3-dimensional representation of the effect of a variation in the feed temperature and feed concentration on the change in flux for Type 1 brine using the 0.45 μm membrane pore size

The 3-dimensional plots clearly show that for both membrane pore sizes investigated, temperature has a far greater influence on permeate flux when compared to feed TDS concentration with an increase in feed temperature resulting in an increase in permeate flux whereas increasing feed concentration had little to no effect on the permeate flux. This trend was observed for both the GVHP (0.22 μm) and HVHP (0.45 μm) membrane pore sizes for the treatment of Type 1 brine.

Figure 11 and Figure 12 shows the permeate flux as a function of feed temperature as well as the vapour pressure on the secondary y-axis at different concentration levels for Type 1 brine using 0.22 μm and 0.45 μm pore size membranes respectively. Raoult's Law was used to determine the vapour pressure driving force at the different feed concentrations and feed temperatures for the prepared NaCl Type 1 brine. The data point, presented at 65 g/L feed concentration and 60°C feed temperature in Figure 11, is significantly lower and deviates from the observed trend hence it can be stated that it was an outlying data point.

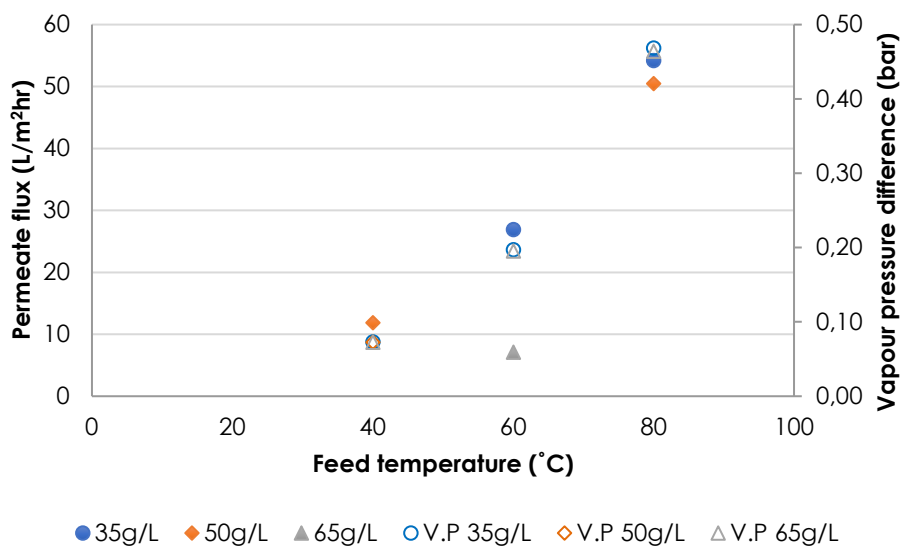


Figure 11: Change in flux rate with a change in feed temperature at different feed concentration levels for the treatment of Type 1 brine using the 0.22 μm membrane pore size

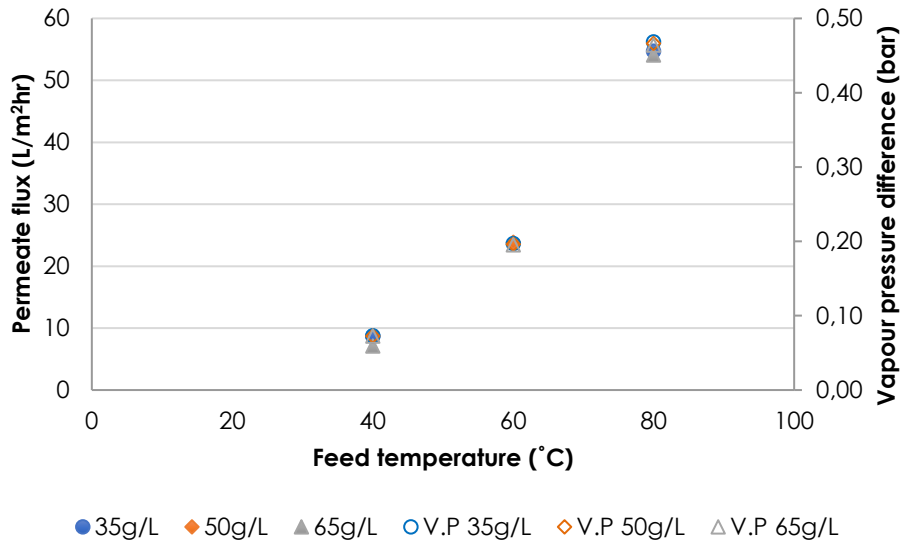


Figure 12: Change in flux rate with a change in feed temperature at different feed concentration levels for the treatment of Type 1 brine using the 0.45 μm membrane pore size

Both the 0.22 μm and 0.45 μm pore size membranes displayed similar performance at the same operating conditions and also responded the same to an increase in feed temperature. As the feed temperature increased, the two membrane pore sizes exhibited higher flux rates, which indicates that the pore sizes studied were appropriate and did not limit the vapour pressure driving force increase because of an increase in feed temperature. Also, the fluxes closely matched the vapour pressure trends for both membranes as expected. The vapour pressure at the different concentration levels are almost identical which further supports the observation that concentration at the lower TDS levels showed no impact on the flux rate.

4.2.2.2 Development of permeate flux model for Type 1 brine

The Design Expert 11 software was used to analyse the measured response of permeate flux of NaCl.H₂O solution at varying feed concentrations (35, 50 and 65 g/l), feed temperatures (40°C, 60°C and 80°C) and membrane pore sizes (0,22 μm and 0,45 μm). The significance test for the regression models and individual model coefficients was determined for all responses using the ANOVA statistical software package. The analysis of variance for the flux quadratic model can be seen in Table 12 and shows the significant model terms affecting the flux decline.

Table 12: ANOVA response for the Quadratic model using Design Expert 11 for Type 1 brine

Source	Sum of squares	df	Mean Square	F-value	P-value	
Model	11838,20	8,00	1479,78	358,07	<0,0001	Significant
A-Feed temperature (°C)	9583,73	1,00	9583,73	2319,06	<0,0001	
B-Concentration (g/L)	11,15	1,00	11,15	2,70	0,1154	
C-Membrane pore size (µm)	4,62	1,00	4,62	1,12	0,3024	
AB	0,55	1,00	0,55	0,13	0,7185	
AC	20,22	1,00	20,20	4,89	0,0383	
BC	3,93	1,00	3,93	0,95	0,3407	
A2	223,04	1,00	223,04	53,97	<0,0001	
B2	7,75	1,00	7,75	1,88	0,1853	
Residual	86,78	21,00	4,13			
Lack of fit	13,86	1,00	13,86	0,065		Not significant
Pure Error	72,92	20,00	3,65			
Cor Total	11924,99	29,00				

Source	Adjusted R ²	Predicted R ²
Quadratic	0,99	0,9854

Both R² and R²-adjusted values were also presented which indicated the degree of fit, defined as the ratio of the explained variation to the total variation. The analysis suggested a good model fit should be at least 0.9854 for R². The adjusted-R² value was found to be 0.9900, which is a difference of less than 0.2, suggesting that the quadratic model was a good fit for the data. The P-value was lower than 0.05 which means the model term is significant. An F-value of 358.07 implies the model is significant since there is only a 0.01% chance that an F-value this large could occur due to noise. According to the model, feed temperature is significant and has the greatest influence on the response, i.e. permeate flux.

Equation 16 below shows the final model in terms of coded factors. A represents the feed temperature (°C), B represents the feed concentration (g/L), and C represents the pore size (µm):

$$flux = 22.55 + 22.98A - 0.7837B + 0.4363C - 0.2046AB + 1.05AC + 0.4652BC + 6.26A^2 + 1.17B^2 \quad (16)$$

Final equations in terms of actual factors can be seen for each pore size investigated. For Equations 17 and 18, T represents the feed temperature (°C), and C represents the feed concentration (g/L):

$$flux_{GVHP,0.22} = 27.81439 - 0.748949T - 0.561393C - 0.000682TC + 0.015660T^2 + 0.005191C^2 \quad (17)$$

$$flux_{HVHP,0.45} = 19.25581 - 0.643455T - 0.499364C - 0.000682TC + 0.015660T^2 + 0.005191C^2 \quad (18)$$

The equation in terms of actual factors can be used to make predictions about the response for given levels of each factor. Here, the levels are specified in the original units for each factor. The coded equation, Equation 10, was useful for identifying the relative impact of the factors by comparing the factor coefficients.

The permeate flux data obtained from running the test runs were evaluated by plotting the normal probability (%) against the externally studentized residuals as seen in Figure 13 below. The linear line of fit observing the relationship between normal probability and externally studentized residuals is appropriate. A good fit means that no response transform was required, and the normality of the data did not experience any specious problem.

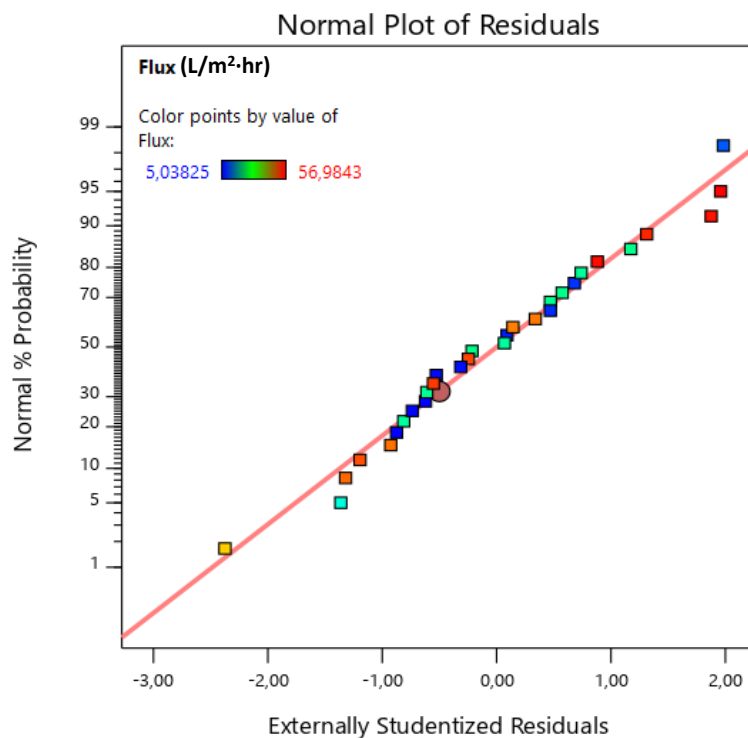


Figure 13: Normal plot of residuals for Type 1 brine flux model

The relationship between the actual and the predicted values are shown in Figure 14, which indicates that the developed model was acceptable for the prediction of permeate flux since the predicted values were very close to the actual experimental values.

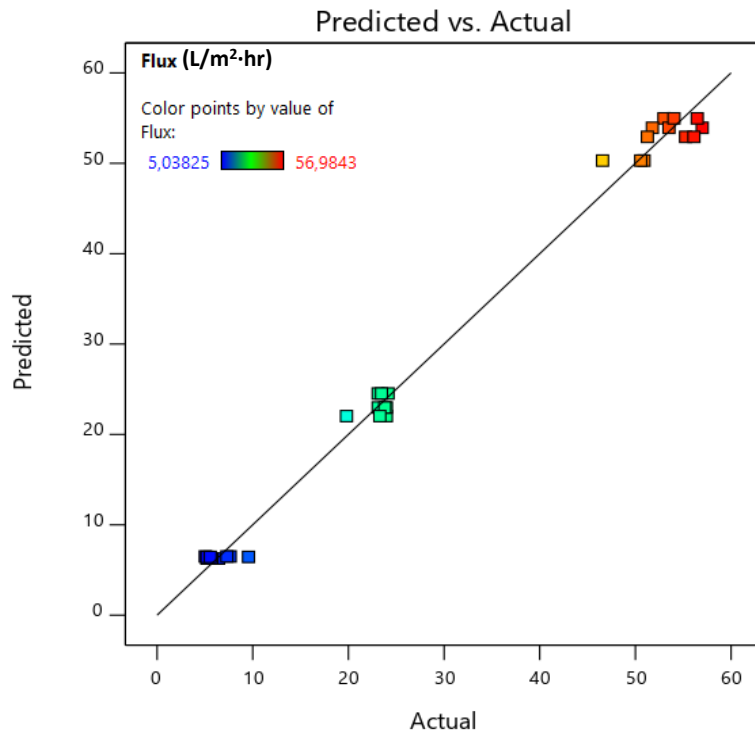


Figure 14: Predicted values vs Actual values

4.2.2.3 Effect of process parameters on permeate flux for the treatment of Type 1 brine

The purpose for predicting the permeate flux was to develop a model, to assist in the selection of a suitable range for process optimisation. The permeate flux observed during the experimental runs was directly related to the process parameters investigated, providing some interaction effect.

Figure 15 shows a perturbation plot displaying the effect of concentration and feed temperature on permeate flux for both pore size membranes.

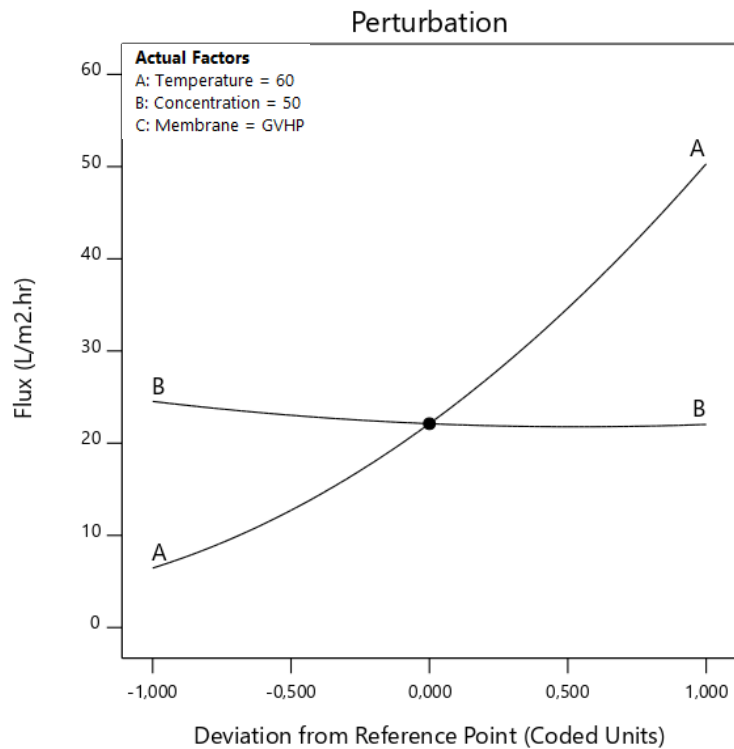


Figure 15: Perturbation plot of factor interaction for GVHP membrane for the treatment of Type 1 brine

A perturbation plot allows for a comparison of the effect of factors at a certain point in the design space, however it does not show the effect of interactions of the factors. The points selected to represent factors A and B in Figure 15 is feed temperature at 60°C and feed concentration at 50 g/L. Factor C represents the pore size of the membrane used (GVHP_{0.22} μm). The primary factor that affected the permeate flux for Type 1 brine when using MD, appeared to be feed temperature. The effect of concentration was not significant according to the perturbation plot above.

5 Investigating the effect of membrane characteristics on MD performance for Type 2 prepared brine and real world industrial brine

Chapter 6 focussed on the effect of Type 1 Brine – a monovalent ion dominant, non-scaling/fouling brine on the MD performance as a function of membrane characteristics. This chapter focusses on the effect that Type 2 Brines, i.e. divalent and trivalent ion dominant brines with significant scaling and/or fouling potential have on the MD performance as a function of membrane characteristics. The investigation looked at Type 2 prepared brines as well as an actual real life industrial Type 2 brine.

5.1 Investigation on Type 2 Prepared Brine

5.1.1 Experimental methodology for investigation on Type 2 prepared brine

This experiment investigated the effect that membrane pore size, increasing feed concentration and operating conditions had on MD performance for Type 2 Brines.

The process conditions for this experiment were as follows:

Brine used: Prepared Type 2 brine

Brine composition: The composition of the prepared Type 2 brine investigated in this study is shown in Table 7 and Table 8 and Table 8.

Feed TDS concentrations of prepared Type 2 brines: 11870 mg/L and 27025 mg/L

Temperature: $T_{\text{feed}} = 40^{\circ}\text{C}$, 60°C , 80°C and $T_{\text{perm}} = 10^{\circ}\text{C}$

Flowrates: $F_{\text{feed}} = 130 \text{ L/hr}$

Run time: 3 hours

The experimental matrix used for this experiment is shown in Table 13:

Table 13: Experimental matrix used to investigate the effect of membrane characteristics on MD performance for Type 2 brine

Test Number	Pore Size (μm)	Feed Temperature ($^{\circ}\text{C}$)	Product Temperature ($^{\circ}\text{C}$)	ΔT ($^{\circ}\text{C}$)	Feed and product flow rate (L/hr)	Synthetic brine concentration (mg/L)
1	0.22	40	10	30	130	11870
2	0.45	40	10	30	130	11870
3	0.22	60	10	50	130	11870
4	0.45	60	10	50	130	11870
5	0.22	80	10	70	130	11870
6	0.45	80	10	70	130	11870
7	0.22	40	10	30	130	27025
8	0.45	40	10	30	130	27025
9	0.22	60	10	50	130	27025
10	0.45	60	10	50	130	27025
11	0.22	80	10	70	130	27025
12	0.45	80	10	70	130	27025

5.1.2 Results and discussion on the investigation on the effect of membrane characteristics on MD performance for Type 2 prepared brine

This experiment investigated the effect that membrane pore size, increasing feed concentration and operating conditions for Type 2 Brine had on MD performance. A summary of the flux rates and salt rejection of all the 180-minute test runs for the treatment of the prepared Type 2 brine is presented in Table 13 below:

Table 14: Summary of experimental run results of the prepared Type 2 brine

Feed TDS (mg/L)	Membrane pore size (μm)	Ave. flux ($\text{L}/\text{m}^2\cdot\text{hr}$)	Salt Rejection (%)
11870	40°C feed temperature		
	0.22	11,39	99,97
	0.45	11,06	99,94
	60°C feed temperature		
	0.22	19,04	99,96
	0.45	25,11	99,97
	80°C feed temperature		
	0.22	48,04	99,97
	0.45	40,13	99,97
	27025	40°C feed temperature	
0.22		7,56	99,98
0.45		12,60	99,99
60°C feed temperature			
0.22		15,18	99,99
0.45		15,90	99,99
80°C feed temperature			
0.22		28,67	99,98
0.45		26,17	99,98

Table 13 shows that a flux rate increase of 4.2 times and 3.63 times was observed when increasing the feed temperature from 40°C to 80°C for the 0.22 μm and 0.45 μm membrane pore sizes respectively. This is a significant in flux rate for temperatures that can be achieved using waste heat and renewable energy sources such as solar heat.

Figure 16 shows the effect of feed temperature for the treatment of prepared Type 2 brine using membranes with 0.22 μm and 0.45 μm pore sizes. The chemical composition of the prepared Type 2 brine used for this run can be seen in Table 7.

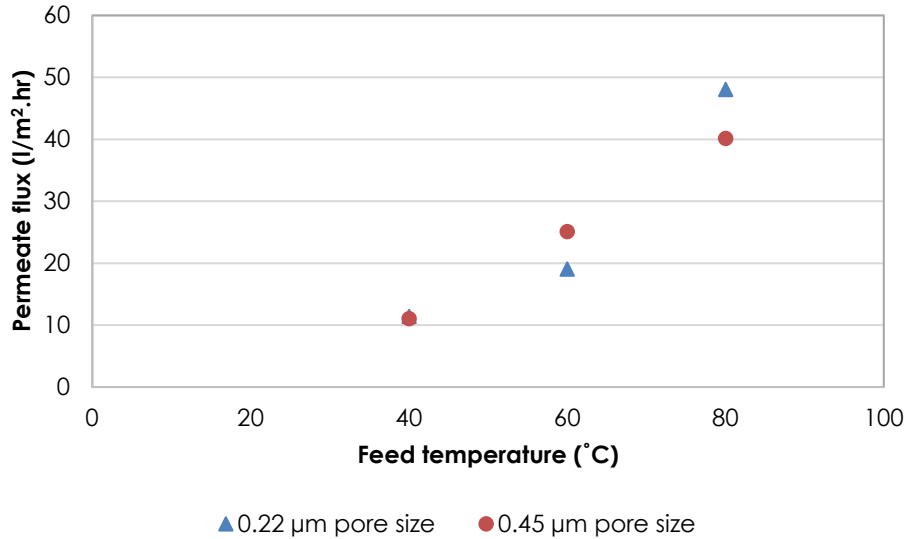


Figure 16: Effects of feed temperature on flux rate for the treatment of prepared Type 1 brine (Initial feed TDS 11870 mg/L) using a 0.22 µm and 0.45 µm pore size membrane

The general trend for both membranes was that an increase in feed temperature resulted in an increase in flux rate. This is explained by the fact that the vapour pressure difference is the main driving force for the mass transfer and that vapour pressure difference and flux rate are directly proportional. At 40°C the driving force was too low and yielded a flux rate below the minimum 18 L/m²-hr required to ensure commercial viability when compared to MED or MVC.

The results confirmed that when keeping the material type and other characteristics constant besides pore size, membranes with larger pore size have higher flux and also higher wetting tendency. The larger, 0.45 µm pore size membrane, yielded higher flux until wetting occurs. This relationship can be attributed to the change of mass transfer modality from Knudsen diffusion to Knudsen-Poiseuille type according to the Kinetic theory of gases (Bhattacharya et al., 2014). Viscous flow starts and eventually dominates the mass transfer mechanism if the average pore size is bigger than the mean free path of the molecules. This causes an increase in diffusion of the vapour and ions in the feed to the product side which results in a higher wetting tendency. LEP and contact angle appear more significant when considering the maximum pore size of the membrane. A smaller maximum pore diameter has a greater impact on the LEP (Damtie et al., 2018).

To determine the effects that a change in feed concentration has on the flux rate, two prepared Type 2 brine solutions of varying concentrations were prepared and investigated with the 0.22 µm and 0.45 µm membrane pore sizes. The chemical makeup of the two varying feed TDS concentration 11870 mg/L and 27025 mg/L prepared Type 2 brines can be seen in

Table 7 and Table 8 respectively. The feed temperature for these test runs were set to 60°C and the product temperature was set to 10°C.

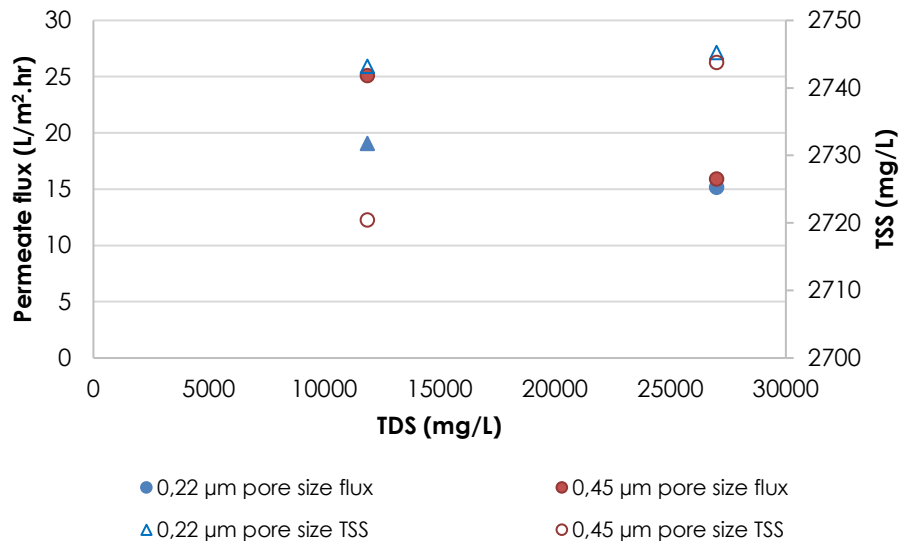


Figure 17: Effects of feed concentration and suspended solids for the treatment of prepared Type 2 brine using 0.22 µm (GVHP) and 0.45 µm (HVHP) membrane pore size

According to Raoult's Law, the vapour pressure is negligibly affected by the amount of solute in the solution but rather based on the solvent molal concentration particularly where the solvent molal concentrations for the concentrated solutions are all above 99%.

Therefore, the observed 30% decline in flux between the lower TDS variant Type 2 brine and the higher TDS variant on in Figure 17 can only be assumed to be due to scaling/fouling phenomena as the initial brine would need to be concentrated 60 times for the concentration to have a 10% effect on the vapour pressure according to Raoult's Law.

The calculated aqueous thermodynamic equilibrium solubility based TSS versus flux plot in Figure 17 shows that the increase in TSS as the feed concentration increases, has a negative effect on the flux.

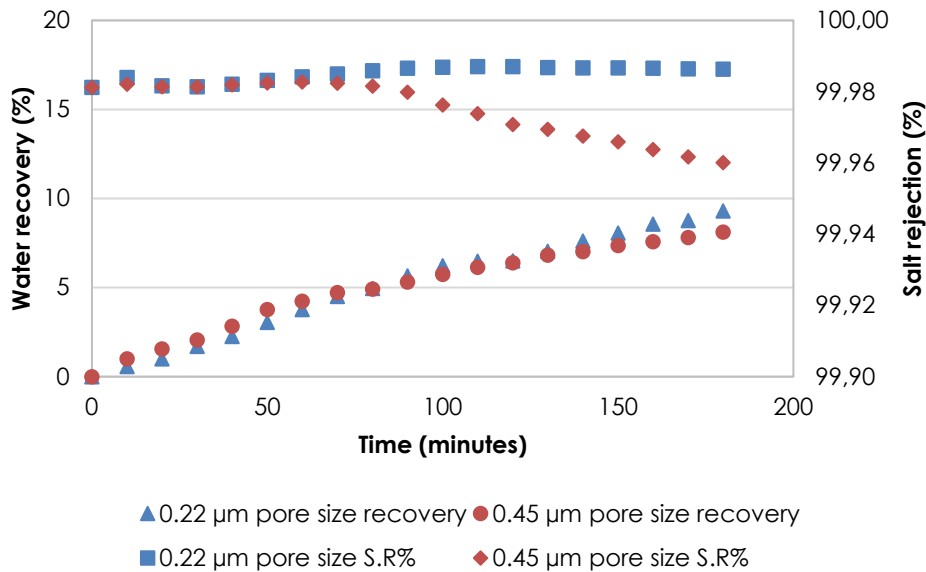


Figure 18: Effects of time (increase in feed concentration and suspended solids) on the water recovery and salt rejection for the treatment of prepared Type 2 brine using 0.22 µm (GVHP) and 0.45 µm (HVHP) membrane pore size

Figure 18 shows that approximately 50 minutes into the experiment using the prepared 27025 mg/L Type 2 brine, the larger 0.45 µm membrane pore size began to experience wetting due to scaling/fouling.

The high vapour pressure driving force as a result of an increase in feed temperature to 80°C yielded higher flux but also accelerated the wetting tendency since the rate of fouling increased. The 0.22 µm membrane pore size displayed higher salt rejection results over the duration of the experiment.

5.2 Investigation on real-world industrial brine

5.2.1 Experimental methodology for investigation using real-world industrial brine

This experiment aimed to determine the ideal membrane pore size and operating conditions for Type 2 Brine using MD under specific operating conditions of feed temperature and feed water concentration for brine emanating from mining and industrial wastewater. This study also focussed on establishing the effect that increasing feed TDS concentration had on the performance of the membrane distillation system using the commercially available membrane distillation membranes, GVHP and HVHP.

As shown in Table 15 based on the feed water composition, this water was classified as Type 2 brine because it comprised monovalent and divalent species and furthermore had a scaling/fouling tendency as evidenced by the scaling indices shown in Table 16.

Table 15: Water analysis data for the real brine emanating from industrial wastewater used for Experiment 7

Component	Concentration (mg/L)
Ca ²⁺	98,01
Mg ²⁺	107,93
Na ⁺	1131,28
K ⁺	25
Fe ³⁺	0,79
Mn ²⁺	0,79
SO ₄ ²⁻	424,58
Cl ⁻	1793,54
HCO ₃ ⁻	263,09
CO ₃ ²⁻	1,75
CO ₂	0,84

Table 16: Scaling indices for real brine used in Experiment 7

Scalant Type	(%)
CaCO ₃	121,64
Fe(OH) ₃	920,58
Mn(OH) ₂	306,86

The process conditions for Experiment 7 were as follows:

Brine used: Real industrial brine

Temperature: T_{feed} = 60°C and T_{perm} = 10°C

Flowrates: F_{feed} = 130 L/hr

Run time: 3 hours

5.2.2 Results and discussion on the effect of pore size on the performance of MD using real industrial brine emanating from an RO process

The results for this experiment, which investigated the effect of real brine emanating from an RO process on the performance of MD is shown in Table 17 below. This experiment was performed at a feed and permeate temperature of 60°C and 10°C respectively, using the 0.22 µm and 0.45 µm pore size membrane for an 8-hour period.

Table 17: Results for real brine after running system for 480 minutes

Membrane	Membrane pore size (μm)	Average Flux ($\text{L}/\text{m}^2\cdot\text{hr}$)	Salt Rejection (%)
GVHP	0.22	18,89	99,97
HVHP	0.45	14,33	99,95

The flux obtained after 480 minutes was 18.89 $\text{L}/\text{m}^2\cdot\text{hr}$ and 14.33 $\text{L}/\text{m}^2\cdot\text{hr}$ for the 0.22 μm and 0.45 μm pore size membranes respectively. The final water recoveries achieved for the 0.22 μm and 0.45 μm pore size membranes were 16.4% and 12.4% respectively. It is important to note that whilst the recovery percentages appear to be low, this is for a single element MD module, whereas a MD process would comprise multiple modules in series resulting in an increase in overall recovery.

The results in Table 17 show that with the real industrial Type 2 brine, the 0.22 μm pore size membrane yielded a slightly higher flux when compared to the prepared lower TDS variant Type 2 brine with a feed TDS of 11870 mg/L. Furthermore, the flux observed was significantly higher than prepared higher TDS variant Type 2 brine with a feed TDS of 27025 mg/L under the same conditions.

The 0.45 μm membrane on the other hand performed similarly to the prepared higher TDS variant Type 2 brine with 27025 mg/L feed TDS. No major flux decline was observed when comparing the 180-minute run to the 480-minute run.

A possible reason for the larger 0.45 μm pore size membrane performing worse in this experiment could be due to the particle size of the suspended solids in the real brine solution being too small. This may have resulted in particles being small enough to enter the larger 0.45 μm pore size membrane which would have caused wetting.

In conclusion, the investigations into the effects of membrane pore size, transmembrane temperature differential and feed water characteristics on the resultant flux rate characteristics for prepared Type 2 brine yielded the following results:

- i) For the 0.22 μm and 0.45 μm pore size membranes, increase in feed temperature from 40°C to 80°C for prepared Type 2 brine with an initial feed TDS of 11870 mg/L led to flux increases of approximately 4.2 and 3.6 times respectively.
- ii) The maximum fluxes obtained for the 0.22 μm pore size membrane at feed TDS concentrations of 11870 mg/L and 27025 mg/L and 80°C were 48.03 $\text{L}/\text{m}^2\cdot\text{hr}$ and 28.67 $\text{L}/\text{m}^2\cdot\text{hr}$ respectively. Hence, the 0.22 μm pore size membrane generally performed better in these experiments
- iii) The maximum fluxes obtained for the 0.45 μm pore size membrane at feed TDS concentrations of 11870 mg/L and 27025mg/L and 80°C were 40.13 $\text{L}/\text{m}^2\cdot\text{hr}$ and 26.17 $\text{L}/\text{m}^2\cdot\text{hr}$ respectively.

6 Scaling/fouling effects on MD performance and the development of an algorithm to determine the suitability of MD for the treatment of brines

This chapter focusses on the effects, if any, of scaling/fouling on the performance of the MD system using commercially available MD membranes, for the treatment of Type 1 and Type 2 prepared brines. Furthermore, the final part of this chapter focusses on the integration of the research findings in the preceding chapters towards the development of an algorithm for use as a technology pre-selection tool by industrial practitioners to determine the potential suitability of MD for the treatment of any particular brine.

6.1 Scaling/fouling effects on MD performance

6.1.1 Scaling/fouling effects on MD performance for prepared Type 1 brine

6.1.1.1 Experimental Methodology

The aim of this experiment was to determine the effects if any of scaling/fouling on the performance (focussed on membrane flux, water recovery and water purity) of the MD system using the commercially available MD membranes, for the treatment of Type 1 brine. Theoretically, by definition, Type 1 brines in this study were classified as non-scaling or those with little to no scaling potential.

The experimental duration was 6 hours at a feed temperature of 60°C, with volume readings being taken at 30-minute intervals. The experimental matrix for this experiment is shown in Table 18 below:

Table 18: Experimental Matrix

Test #	Feed temperature [°C]	NaCl concentration [g/L]	Membrane	Pore Size [µm]
1	60	200	GVHP	0.22
2	60	200	HVHP	0.45

The initial feed TDS being selected as high as it was for this experiment at 200 g/L was due to the relatively high solubility of NaCl in water (approximately 360 g/L). This ensured that the initial starting feed TDS concentration below the solubility level but also high enough to determine whether scaling/fouling issues are factor to be taken into consideration when dealing with Type 1 brines.

Table 19: Type 1 Brine (NaCl) concentration level used

Chemicals	Molecular weight (g/mol)	Concentration (mg/L)
Sodium Chloride (NaCl)	58,44	200 000

The process conditions for Experiment 4 were as follows:

Brine used: Prepared Type 1 brine

Brine composition: NaCl-H₂O solution: 200 g/L

Temperature: T_{feed} = 60°C and T_{perm} = 10°C

Flowrates: F_{feed} = 130 L/hr

Run time: 6 hours

6.1.1.2 Results and discussion

Table 20 and Figure 19 show a 6-hour long experiment using an initial NaCl concentration of 200 g/L, at feed and permeate temperature of 60°C and 10°C respectively, to compare the performance of the two membrane pore sizes at significantly higher TDS levels that are representative of the concentration at the backend of a system with multiple modules in series whilst still below solubility level.

In the event that the experiment happened to be run to a recovery point that exceeded the solubility limit, then it is assumed that the membrane would begin to undergo scaling/fouling.

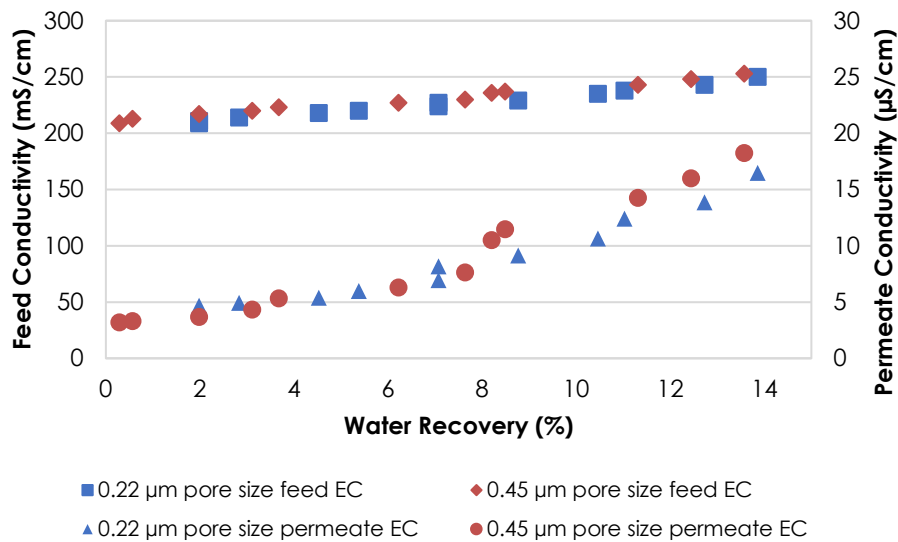


Figure 19: Feed and permeate conductivity as a function of recovery for (6-hour run, 200 g/L initial TDS) prepared Type 1 brine using 0.22 µm pore size and 0.45 µm pore size membranes

Table 20: Permeate flux rate of Experiment 4 to determine the effect of scaling/fouling for prepared Type 1 brine

Membrane	Membrane pore size (µm)	Permeate Flux (L/m ² -hr)
GVHP	0.22	25,54
HVHP	0.45	20.85

For this experiment, no significant flux was observed up to the 6th hour, which was the duration of test.

The 0.22 µm pore size membrane yielded a flux 22.5% higher than the 0.45 µm pore size membrane at these conditions.

Figure 20 shows the results of the investigation aimed at determining the effects that scaling/fouling if any had on the performance of the MD system for Type 1 brine.

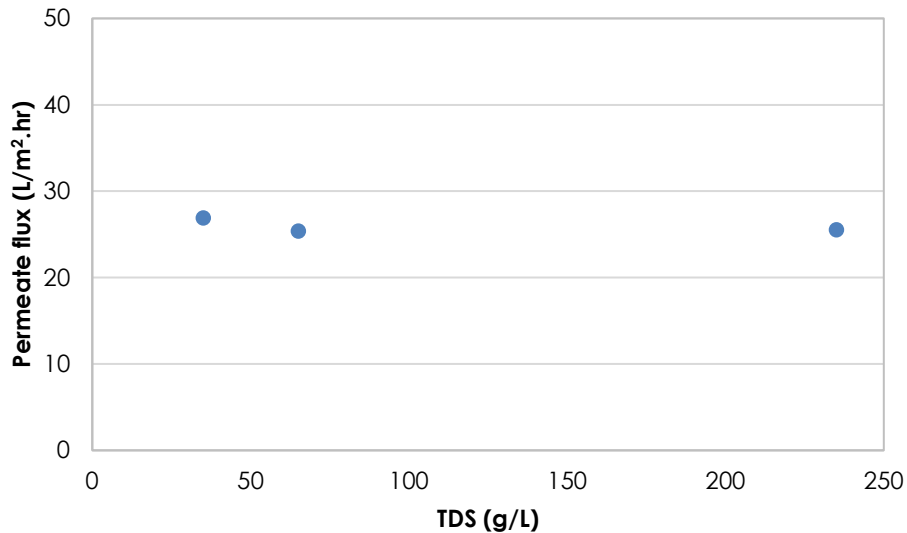


Figure 20: Effects of concentration on flux rate for the treatment of Type 1 brine

Figure 20 shows that there was an insignificant reduction in the permeate flux across the concentration range (65 g/L to 235 g/L) investigated. This is to be expected and is in agreement with Raoult's Law, which predicts that the vapour pressure is less affected by the amount of solute in the solution and more affected by the solvent molal concentration. As the solvent molal concentrations for the concentrated solutions are all above 99%, the vapour pressure is not expected to change significantly for the Type 1 brine used in Experiment 4. Furthermore, as Type 1 did not exhibit any scaling/fouling characteristics, no flux reduction was observed due to suspended solids as there were none.

Although the 0.22 μm and 0.45 μm membrane pore sizes showed very little difference in performance in Experiment 3, the observation in Experiment 4, which had a significantly higher initial feed TDS, was that the smaller 0.22 μm pore size membrane performed significantly better in terms of flux.

The final conductivity of the test run for the 0.22 μm pore size membrane was approximately 10% lower than the 0.45 μm pore size membrane showing that the 0.22 μm pore size membrane yielded better flux and water purity.

In summary, the investigations into the effects of membrane pore size, transmembrane temperature differential and feed water characteristics on the resultant flux rate and scaling/fouling characteristics for prepared Type 1 brine yielded the following results:

- i) For the 0.22 μm and 0.45 μm pore size membranes, increase in feed temperature from 40°C to 80°C led to flux increases of approximately 4.6 and 7.7 times respectively
- ii) The maximum fluxes obtained for the 0.22 μm and 0.45 μm pore size membranes at 80°C were 54.2 L/m²·hr and 54.7 L/m²·hr respectively. At a feed temperature of 40°C, the fluxes were below the minimum 18 L/m²·hr for both membrane pore sizes

- iii) Changes in feed concentration for the monovalent solutions did not have any significant effect on MD performance, which was largely attributed the non-scaling/fouling characteristics of the brine
- iv) The 0.22 μm pore size membrane yielded a flux which was 22.5% higher than that achieved of the 0.45 μm pore size membrane over a longer duration and at a very high TDS feed concentration.

6.1.2 Scaling/fouling effects on MD performance for Type 2 prepared brine

6.1.2.1 Experimental Methodology

The aim of this experiment was to determine the effects of scaling/fouling on the performance (focused on membrane flux, water recovery and water purity) of the MD system using the commercially available MD membranes, for the treatment of prepared Type 2 brine.

These experiments were allowed to run for as long as there was enough solution for a volume reading to be taken.

The total suspended solids concentration (TSS) was measured during these experiments to determine the TSS concentration at which the suspended solids start to impact negatively on the overall system performance.

The process conditions for Experiment 6 were as follows:

Brine used: Prepared Type 2 brine

Brine composition: The composition of the prepared Type 2 brine investigated in this study is shown in Table 8.

Feed TDS concentrations of prepared Type 2 brines: 27025mg/L

Temperature: $T_{\text{feed}} = 60^{\circ}\text{C}$ and $T_{\text{perm}} = 10^{\circ}\text{C}$

Flowrates: $F_{\text{feed}} = 130 \text{ L/hr}$

6.1.2.2 Results and Discussion

This experiment was performed at 60°C feed temperature and 10°C permeate temperature to determine the effect of scaling/fouling resulting from a dynamic increase in the feed water concentration and increasing suspended solids on the MD system performance. The experiment was run using 4 L of the prepared Type 2 brine with an initial feed concentration of 27025 mg/L, until either the feed solution's volume change could no longer be measured because there was very little solution left or because the flux reduced significantly due to scaling/fouling.

Initially, the total suspended solids (TSS) concentration in the solution was measured every hour throughout the 12-hour long experiment using the conventional gravimetric analytical method involving sample collection, filtration, drying and weighing. However, owing to the relatively small sample that

could be extracted from the reactor relative to the standard 1 litre sample that is typically used when determining TSS, the TSS results obtained showed some inaccuracies. Consequently, an aqueous thermodynamic modelling simulation using OLI Stream Analyzer Version 10 software was used to predict the theoretical TSS based on the dynamic equilibrium solubilities of all the aqueous species in solution as the volume in the feed reactor and consequently the feed concentration changed over time.

Table 12 summarises the results obtained from the scaling/fouling effects experiment for the treatment of prepared Type 2 (feed TDS 27025 mg/L) brine using the 0.22 μm and 0.45 μm pore size membranes

Table 21: Summary of results for scaling/fouling experiments using the prepared Type 2 brine

Membrane pore size (μm)	Average Flux ($\text{L}/\text{m}^2\text{-hr}$)	Salt Rejection (%)	Recovery (%)	Cumulative permeate volume (mL)	Running time (hrs)
0.22	10,58	99,93	38,17	1526,85	35,0
0.45	23,10	99,97	55,14	2205,45	24,0

The average flux rate and TSS as a function of water recovered from the feed can be seen in Figure 21 and Figure 22 for the 0.22 μm and 0.45 μm pore size membranes respectively. The flux rates represented are the average fluxes for the water recovery ranges, 0-10%, 11-20%, 21-30%, 31-40% and 41-50%.

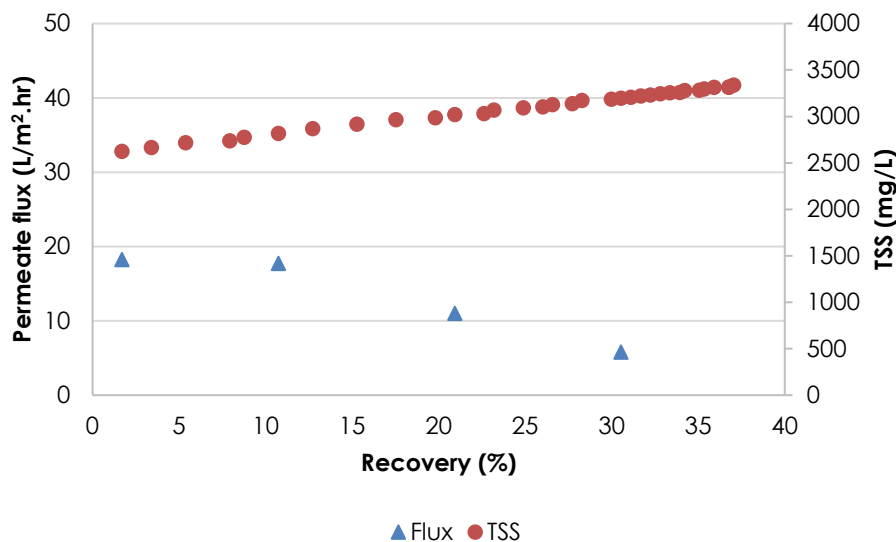


Figure 21: Flux rate and TSS as a function of water recovery for prepared Type 2 brine using the 0.22 μm pore size membrane

For the 0.22 μm pore size membrane, the flux appears to be consistent up to 10% water recovery, after which it starts to drop off as seen in Figure 21. This is due to the fact that as the water transfer across the membrane by evaporation increases, the feed becomes increasingly concentrated, reaches and

exceeds the solubility of various species, which in turn crystallise out increasing the TSS in the feed reactor. These solids deposit onto the membrane surface, resulting in membrane scaling and flux decline.

The active membrane surface area is reduced due to a build-up of crystals which means less water can be transferred. The flux declined from an average initial of 15 L/m²·hr to an average of approximately 5 L/m²·hr. This went on for a further 17 hours at which point the flux rate decline to 2.61 L/m²·hr with a total water recovery of 38.74%. The run was allowed to run until volume level readings could no longer be taken, which occurred after 35 hours of running time. The average flux for the 0.22 µm during this run was 10.58 L/m²·hr which is significantly lower than what was observed for the experiments run over a 3-hour period in Experiment 6 using the same initial Type 2 feed brine concentration.

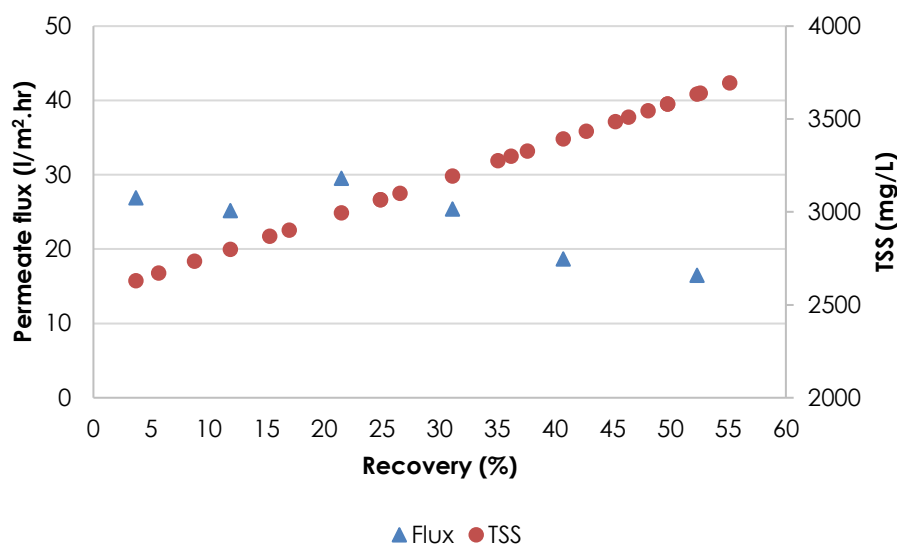


Figure 22: Flux rate and TSS as a function of water recovery for prepared Type 2 brine using the 0.45 µm pore size membrane

Figure 22 represents significantly better results for the 0.45 µm pore size membrane when comparing it to the 0.22 µm pore size membrane. The average flux achieved over the experimental run was 23.1 L/m²·hr which shows that the 0.45 µm pore size membrane yielded a flux rate 2.2 times greater than that of the 0.22 µm pore size membrane. The running time to achieve the same point at which the 0.22 µm pore size membrane's experiment was stopped only took 24 hours. The water recovery was also 55.14% which was 44.5% more water recovered than what was achieved with the 0.22 µm pore size membrane. Increasing TSS appeared to have minimal effect on the flux rate of the 0.45 µm pore size membrane.

Figure 23 and Figure 24 show the conductivity and TSS as a function of water recovery for prepared Type 2 brine using the 0.22 µm and 0.45 µm pore size membranes respectively. It is clear for both pore sizes that as the water recovery increases, the permeate conductivity and TSS increase as well. The decrease of volume in the feed tank means the water recovery increases, resulting in the feed TDS concentration to increase. This causes more solids to precipitate out and thus the TSS increases.

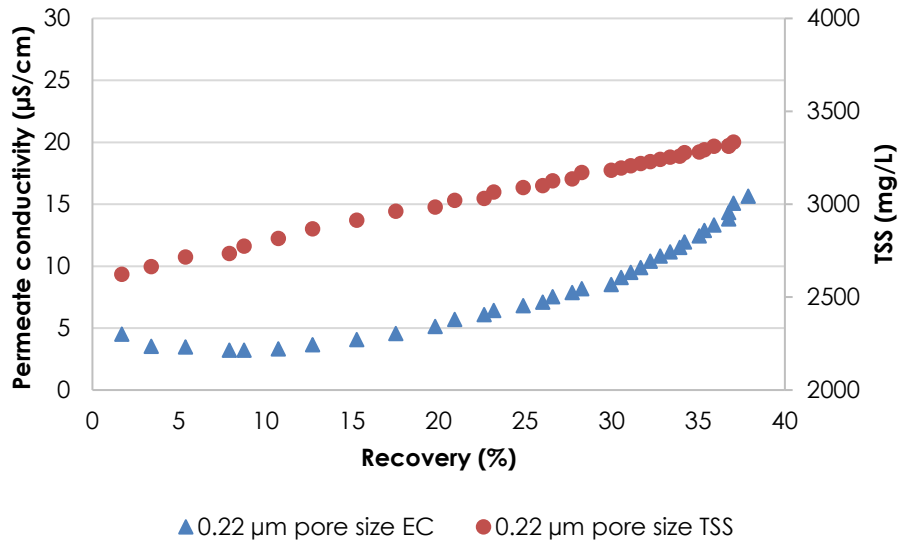


Figure 23: Permeate conductivity and TSS as a function of water recovery for prepared Type 2 brine using the 0.22 µm pore size membrane

The initial product conductivity for the 0.22 µm pore size membrane was 4.52 µS/cm and initially dropped as a result of the permeate from the membrane treatment being purer than the initial EC of the sweep stream in the product tank. After approximately 9% water recovery, the product EC began to increase, and the final EC measurement for the experiment was 15.65 µS/cm indicating that scaling/fouling and pore wetting had occurred, resulting in an increased salt passage through the membrane to the product tank.

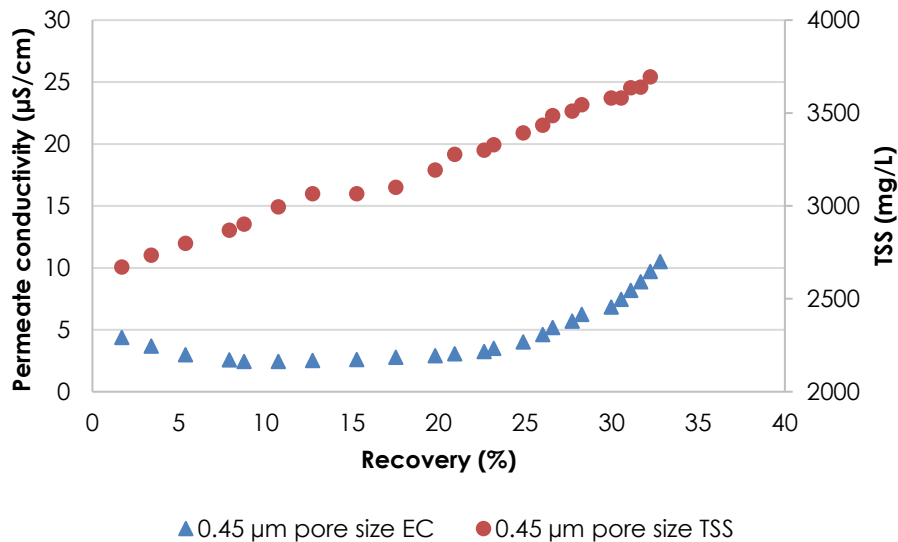


Figure 24: Permeate conductivity and TSS as a function of water recovery for prepared Type 2 brine using the 0.45 µm pore size membrane

Figure 24 showed the initial product conductivity for the 0.45 μm pore size membrane was 4.39 $\mu\text{S}/\text{cm}$ and initially dropped as a result of the permeate from the membrane treatment being purer than the initial EC in the sweep stream in the product tank. The EC began increasing at a significantly higher water recovery of approximately 30% and the final EC measurement for the experiment was 10.52 $\mu\text{S}/\text{cm}$. The increase in permeate EC was much less substantial for the 0.45 μm pore size membrane when compared to the water quality of the product water from the 0.22 μm pore size membrane experiment.

Figure 25 and Figure 26 show the salt rejection and TSS as a function of water recovery for prepared Type 2 brine using the 0.22 μm and 0.45 μm pore size membranes respectively. The plots below give a good indication of the effects of TSS on the salt rejection and the point at which severe scaling/fouling begins to occur.

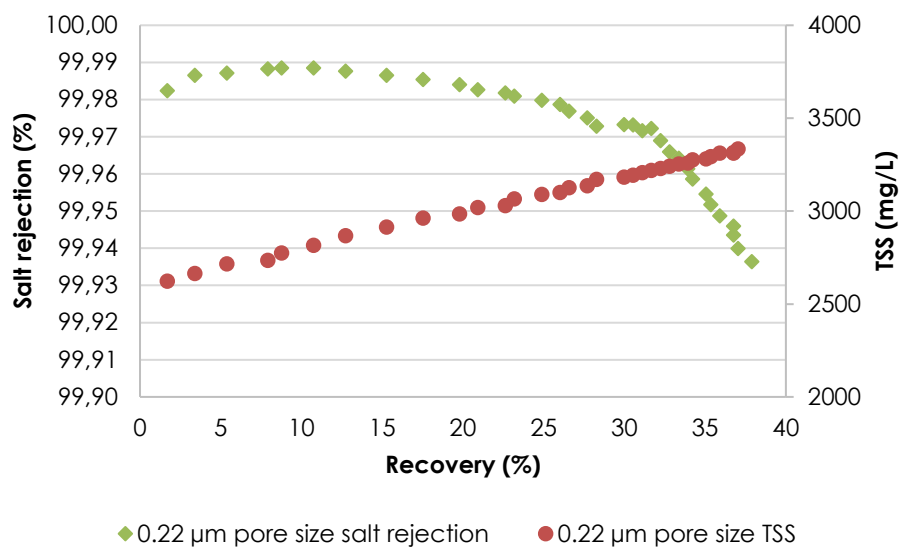


Figure 25: Salt rejection and TSS as a function of water recovery for prepared Type 2 brine using the 0.22 μm pore size membrane

Figure 25 shows that the salt rejection achieved using the 0.22 μm pore size membrane appears to have reached a rejection as low as 99.94% having yielded a salt rejection above 99.98% for over 17 hours and recovery of 27.71%. The salt rejection drops off sharply after approximately 30% recovery and a TSS concentration of 3000 mg/L. Hence, this suggests that the maximum TSS which the system should not exceed using a 0.22 μm pore size membrane is 2900-3100 mg/L. This range factors in the influence that TSS had on the flux rate, the permeate conductivity and the salt rejection.

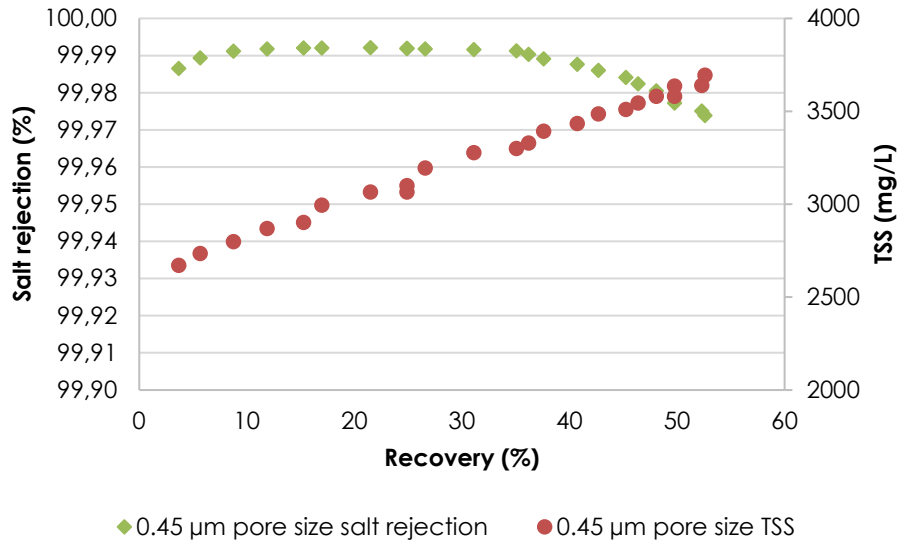


Figure 26: Salt rejection and TSS as a function of water recovery for prepared Type 2 brine using the 0.45 µm pore size membrane

Figure 26 shows that the salt rejection for the 0.45 µm pore size membrane dropped to only 99.97% after over 50% water was recovered and yielded a very rejection of 99.9% for the first 45% of the recovered water. The range at which the maximum TSS which the system should no longer be run a 0.45 µm pore size membrane is 3100-3300 mg/L. This range factored in the influence that TSS had on the flux rate, the permeate conductivity and the salt rejection.

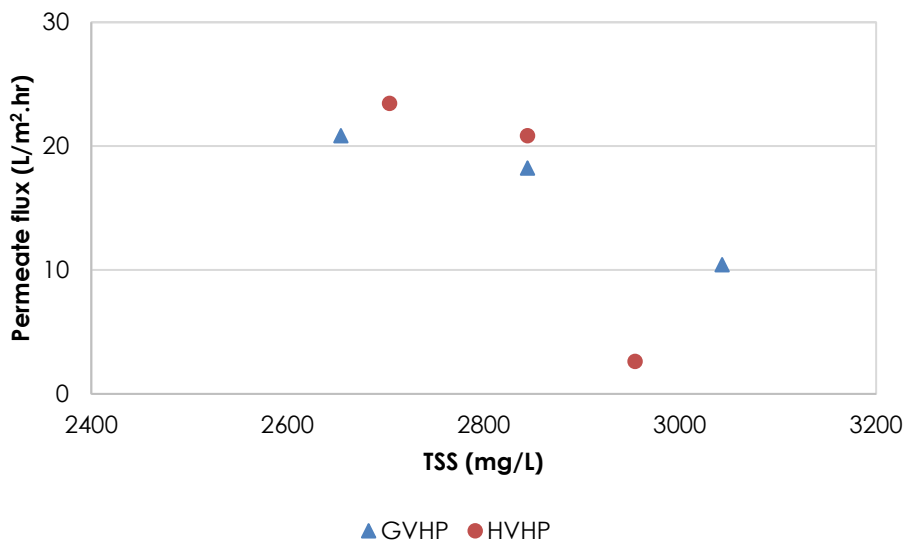


Figure 27: Permeate flux vs Suspended solids in solution

Figure 27 shows the relationship between the total suspended solids (TSS) in the solution and the effect it had on the permeate flux. As anticipated, the trend observed was that as the TSS increased, the permeate flux decreased. The TSS concentration of approximately 2900 mg/L for each membrane pore size appears to have a major detrimental effect on overall system performance in terms of permeate flux. Beyond this TSS and the flux decreases considerably.

In conclusion, the investigations into the effects of membrane pore size, transmembrane temperature differential and feed water characteristics on the scaling/fouling characteristics for prepared Type 2 brine yielded the following results:

- i) Changes in feed concentration for the divalent and trivalent solutions had a significant effect on MD performance, which was largely attributed to scaling/fouling factors as well as the increase of suspended solids present.
- ii) For the larger 0.45 μm pore size performed exceptionally well compared to the 0.22 μm pore size membrane with an increase in feed TSS. The maximum TSS before a sharp decrease in MD performance was experienced for the 0.22 μm and 0.45 μm pore size membranes at 3000 mg/L and 3200 mg/ L respectively.

6.1.3 Effect of particle size on the scaling/fouling effects on MD performance for Type 2 prepared brine

6.1.3.1 Experimental Methodology

The aim of this experiment was to determine whether particle size influenced the scaling/ fouling on MD system performance by adjusting the stirrer speed of the feed tank to 150 rpm, 600 rpm and 1050 rpm. The assumption was that an increase in stirrer speed would cause an increase in shear on the particles causing attrition and breakage resulting in a smaller average particle size. Thus, the effect of particle size could be investigated. The prepared Type 2 brine solution was used for all these experimental runs and the initial TSS was 2550 mg/L.

The system was run at a feed temperature and product temperature of 60°C and 10°C. The experimental procedure described in 0 was used for all three particle size experiments.

The process conditions for this experiment were as follows:

Brine used: Prepared Type 2 brine

Brine composition: The composition of the prepared Type 2 brine investigated in this study is shown in Table 8.

Feed TDS concentrations of prepared Type 2 brines: 27025 mg/L

Temperature: $T_{\text{feed}} = 60^{\circ}\text{C}$ and $T_{\text{perm}} = 10^{\circ}\text{C}$

Feed-side stirrer speed: 150 rpm, 600 rpm and 1050 rpm

Flowrates: $F_{\text{feed}} = 130 \text{ L/hr}$

Run time: 3 hours

6.1.3.2 Results and Discussion

This experiment was based on the assumption was that an increase in stirrer speed would cause an increase in shear on the particles causing attrition and breakage resulting in a smaller average particle size. Thus the effect of particle size could be investigated by increasing the stirrer speed for each sequential run from 150 rpm to 600 rpm and finally to 1050 rpm. The prepared Type 2 brine solution was used for all of these experimental runs and the initial TSS was 2550 mg/L.

Figure 28 shows the effect of particle size, as a result of varying stirrer speed, on the flux rate for the treatment of prepared Type 2 brine using 0.22 μm pore size and 0.45 μm pore size membranes.

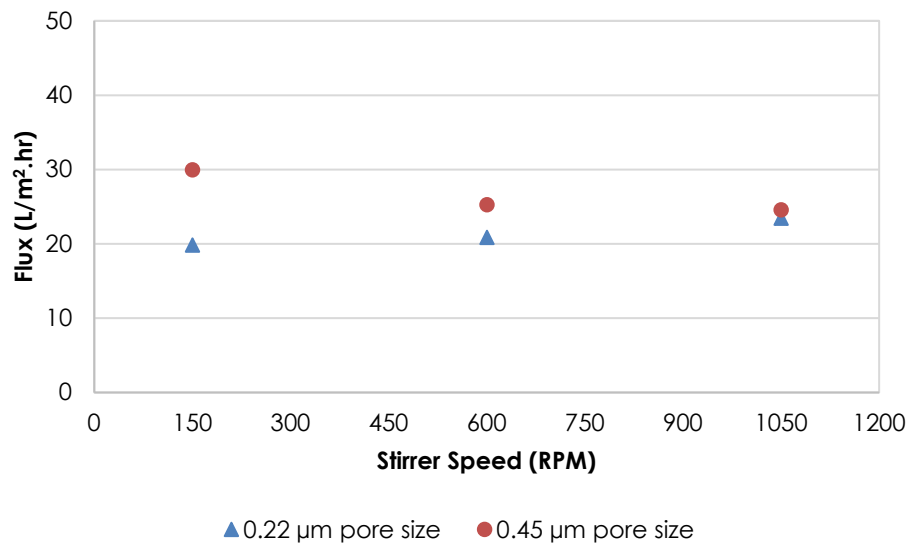


Figure 28: Effect of particle size on the flux rate for prepared Type 2 brine using 0.22 μm pore size and 0.45 μm pore size membranes

An increase in stirrer speed resulted in a decrease in flux for the larger 0.45 μm pore size membrane (HVHP) whereas the opposite was observed for the smaller pore size membrane (GVHP). The trend observed for the 0.45 μm pore size could be attributed to the reduction in particle size at higher impeller speeds, higher shear rates resulting in a smaller overall average particle size that could enter the larger pores of the membrane and thus causing more scaling/fouling.

The smaller, 0.22 μm pore size showed that increasing the stirrer speed resulted in an increase in flux rate. This observation indicates that although the particle size of the solids in the solution are shrinking, the solids in the solution are still larger than the pores of the 0.22 μm pore size membrane but smaller than the pores of the 0.45 μm pore size membrane.

From the results above, it can be concluded that the particle size of the suspended solids in the solution should be bigger so as not to enter the pores of the membrane and cause wetting. Hence, a slower stirrer speed of 150 rpm would yield better MD performance and also improve energy efficiency.

In conclusion, the results of the investigation into the effects of (i) particle size (ii) scaling/fouling characteristics on the resultant flux rate and scaling/fouling characteristics for Type 2 brine can be summarised as follows:

- i) Increasing the impeller stirrer speed in the feed reactor increases the shear on the crystallised particles causing attrition and breakage resulting in a smaller average particle size
- ii) Despite the elevated total suspended solids concentrations, the flux achieved using the 0.45 μm pore size membrane was significantly higher than that for the 0.22 μm pore size membrane.

Furthermore, the flux achieved using the 0.45 μm pore size membrane was greater at lower impeller stirrer speeds suggesting that larger particle sizes which are less likely to enter the membrane pores and cause wetting, promote higher flux rates and should be prioritised in terms of the reactor control.

6.2 Development algorithm to determine membrane distillation suitability towards brine treatment

With the information obtained from the experimental investigations, an algorithm was designed to assist prospective users of membrane distillation technology in better understanding of if and when it is a viable option. This will help gauge industrial demand and requirements to membrane manufacturers which will increase the pool of MD specific membranes available. The algorithm can be seen below in Figure 29.

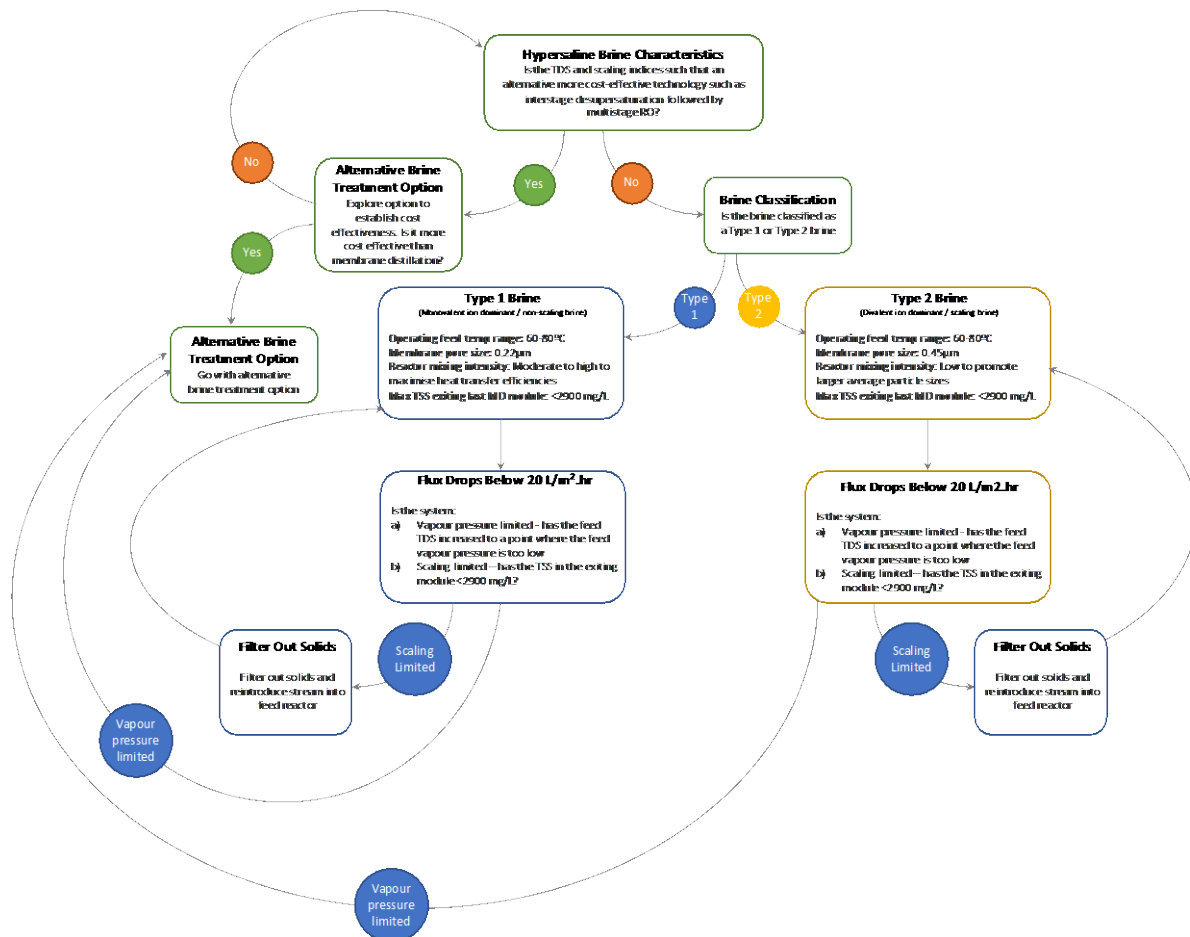


Figure 29: MD Algorithm

The novel MD brine treatment feasibility and process operating conditions algorithm developed in this study provides a useful tool to be used by industry as a preliminary assessment tool when exploring the use of MD as an alternative brine treatment solution and to provide operating parameter guidelines.

7 Conclusions and Recommendations

Of the various membrane characteristics investigated, membrane pore size was identified as the key variable in terms of membrane selection. As a result, the research focussed mainly on two PVDF membranes with pore sizes of 0.22 μm and 0.45 μm .

Two types of brines were investigated: Type 1 Brine, a monovalent ion dominant, non-scaling/fouling brine and Type 2 Brine, which was a divalent and trivalent ion dominant brine with scaling and/or fouling potential. Both types of brines provided the necessary coverage in terms of the variability in brine wastewater characteristics from industrial and mining sectors.

Based on a costing analysis, the minimum flux for an MD process to be cost effective relative to two conventional brine treatment processes, i.e. multi-effect distillation (MED) and mechanical vapour recompression evaporation (MVC) was determined to be 18 L/m²·hr. At fluxes lower than 18 L/m²·hr, MED and MVC appeared to show better commercial viability when compared to MD.

The flux prediction model developed for Type 1 brine (NaCl.H₂O solution) was based on an experimental matrix with the input variables being feed concentration (35, 50 and 65 g/l), feed temperature (40°C, 60°C and 80°C) and membrane pore size (0.22 μm and 0.45 μm). The significance tests for the regression models and individual model coefficients were determined for all responses using statistical methods. The flux prediction models for 0.22 μm and 0.45 μm membrane pore sizes, whose quadratic models showed a very a good data fit are shown below (T represents the feed temperature [°C], and C represents the feed concentration [g/L]):

$$flux_{GVHP,0.22} = 27.81439 - 0.748949T - 0.561393C - 0.000682TC + 0.015660T^2 + 0.005191C^2$$

$$flux_{HVHP,0.45} = 19.25581 - 0.643455T - 0.499364C - 0.000682TC + 0.015660T^2 + 0.005191C^2$$

Additional key findings from the experimental investigation into the effects of membrane pore size, transmembrane temperature differential and feed water characteristics on the resultant flux rate and scaling/fouling characteristics for prepared **Type 1 brine** were as follows:

- i) Temperature had the greatest influence on increasing the permeate flux and that the higher the feed temperature, the higher the flux. At a feed temperature of 40°C, the fluxes were below the minimum 18 L/m²·hr for both membrane pore sizes suggesting that the feed temperatures between 60-80°C would be ideal
- ii) The maximum fluxes obtained for the 0.22 μm and 0.45 μm pore size membranes at 80°C were 54.2 L/m²·hr and 54.7 L/m²·hr respectively. These fluxes were well above the minimum acceptable flux of 18 L/m²·hr for MDC demonstrating potential commercial viability
- iii) Changes in feed concentration for the monovalent solutions did not have any significant effect on MD performance, which was largely attributed to the non-scaling/fouling characteristics of the brine.

This is a major benefit for MDC to be used to treat hypersaline brines at elevated concentrations significantly beyond those capable of being treated by other emerging or commercially available technologies

- iv) At elevated feed total dissolved concentrations (TDS) in excess of 200 g/L, i.e. representing conditions at the tail end of the MDC process, the 0.22 μm pore size PVDF membranes were better suited in terms of achieving a 22.5% higher flux rate (25.54 L/m²·hr) and better salt rejection at higher overall recoveries for Type 1 brines when compared to 0.45 μm pore size membranes.

Similarly, key findings from the experimental investigation into the effects of membrane pore size, transmembrane temperature differential and feed water characteristics on the resultant flux rate and scaling/fouling characteristics for prepared **Type 2 brine** were as follows:

- i) Similar to Type 1 brine, temperature had the greatest influence on increasing the permeate flux and that the higher the feed temperature, the higher the flux.
- ii) The maximum fluxes obtained for the 0.22 μm pore size membrane at feed TDS concentrations of 11870 mg/L and 27025 mg/L and 80°C were 48.03 L/m²·hr and 28.67 L/m²·hr respectively. The maximum fluxes obtained for the 0.45 μm pore size membrane at feed TDS concentrations of 11870 mg/L and 27025 mg/L and 80°C were 40.13 L/m²·hr and 26.17 L/m²·hr respectively. Although, the fluxes for Type 2 brines were lower than those for Type 1 brines owing to the scaling nature of the Type 2 brine and the resultant increase in suspended solids, these fluxes were still above the minimum acceptable flux of 18 L/m²·hr for the commercial viability of MDC
- iii) The 0.45 μm pore size membrane performed significantly better than the 0.22 μm pore size membrane at elevated suspended solids concentrations in terms of permeate flux and salt rejection. However, beyond a suspended solids concentration of 3000 mg/L for the 0.22 μm pore size membranes and 3200 mg/L for the 0.45 μm pore size there was a sharp decline in MD performance both in terms of permeate flux and salt rejection.
- iv) At elevated feed total dissolved concentrations (TDS) and suspended solids concentrations up to 3200 mg/L, 0.45 μm pore size PVDF membranes were better suited in terms of achieving higher flux rates at higher overall recoveries for Type 2 brines.
- v) Despite the elevated total suspended solids concentrations, the flux achieved using the 0.45 μm pore size membrane was significantly higher than that for the 0.22 μm pore size membrane.
- vi) Furthermore, the flux achieved using the 0.45 μm pore size membrane was greater at lower impeller stirrer speeds suggesting that larger particle sizes which are less likely to enter the membrane pores and cause wetting, promote higher flux rates and should be prioritised in terms of the reactor control.

The water purity from all investigations yielded acceptable results and very high rejection (>99.94%) with the product water exhibiting low conductivity (<10 $\mu\text{S/cm}$), which only increased once scaling on the membrane surface and pore wetting caused also caused a decrease in flux rate.

Using the information obtained from the experimental investigations, a decision-making tool was developed to assist prospective users of membrane distillation technology in assessing the viability of

using membrane distillation for brine treatment. Furthermore, the decision-making tool provided guidelines in terms of membrane selection and process operating conditions for specific types of brines.

Although advancements into membrane modifications have accelerated in the past few years, more research needs to go into the development of cheaper membranes for this purpose, since the number of commercially available membranes manufactured specifically for MD use has not increased much.

In conclusion, this study aimed to provide industrial technology developers, suppliers and practitioners with valuable, readily usable information and tools aimed towards considering MDC as an alternative, more energy efficient and sustainable hypersaline brine treatment process towards achieving zero liquid discharge.

References

1. Adnan, S., Hoang, M., Wang, H. & Xie, Z., 2012. Commercial PTFE membranes for membrane distillation application: Effect of microstructure and support material.. *Desalination*, Volume 284, pp. 297-308.
2. Ali, M., Summers, E., Arafat, H. & J.H.L.V.2012., 2012. Effects of membrane properties on water production cost in small-scale membrane distillation systems.. *Desalination*, Volume 306, pp. 60-71.
3. Ali, M., Summers, H. & al., A. e., 2012. Effects of membrane properties on water production cost in small scale membrane distillation systems.. *Desalination*, Volume 306, pp. 60-74.
4. Alkhdhiri, A., Darwish, N. & Hilal, N., 2012. Membrane distillation: A comprehensive review. *Desalination*, 02, Volume 287, pp. 2-18.
5. Alklaibi, A. & Lior, N., 2005. Membrane-distillation desalination: Status and potential. *Desalination*, 171(2), pp. 111-131.
6. Alves, V. & Coelho, I., 2006. Orange juice concentration by osmotic evaporation and membrane distillation: A comparative study.. *Journal of Food Engineering*, Issue 74, pp. 125-133.
7. Anon., n.d.
8. Balasubramanian, P., 2013. A brief review on best available technologies for reject water (brine) management in industries. *International Journal Of Environmental Sciences*, 3(6), pp. 2010-2018.
9. Banat, F. & Simandi, J., 1998. Desalination by Membrane Distillation: A Parametric Study. *Separation Science and Technology*, 33(2), pp. 201-226.
10. Bandini, S. & Sarti, G., 1999. Heat and Mass Transport Resistances in Vacuum Membrane Distillation Per Drop. *AIChE Journal*, 45(7), pp. 1422-1433.
11. Burgoyne, A. & Vahdati, M., 2000. Direct Contact Membrane Distillation. *Separation Science and Technology*, 35(8), pp. 1257-1284.
12. Camacho, L. et al., 2013. Advances in Membrane Distillation for Water Desalination and Purification Applications. *Water*, Volume 5, pp. 94-196.
13. Curcio, E., Criscuoli, A. & Drioli, E., 2001. Membrane Crystallizers. *Industrial Engineering Chemistry Research*, Volume 40, pp. 2679-2684.
14. Curcio, E. & Drioli, E., 2005. Membrane distillation and related operations – review. *Separation & Purification Reviews*, 34(1), pp. 35-36.
15. Dow, N. et al., 2008. *Membrane Distillation of Brine Wastes*, Adelaide: Water Quality Research Australia Limited.
16. Dow, N. et al., 2008. *Membrane Distillation of Brine Wastes*, Adelaide: Water Quality Research Australia Limited.
17. Drioli, E., Ali, A. & Macedonio., 2015. Membrane distillation: Recent developments and perspectives.. *Desalination*, Volume 356, pp. 56-84.

18. EcologyDictionary.org, 2008. *EcologyDictionary.org*. [Online]
Available at: <http://www.ecologydictionary.org/MYPgV/EPA-Terms-of-Environment-Dictionary/BRINE>
[Accessed 23 07 2015].
19. Edward Jones, Manzoor Qadir, Michelle T.H. van Vliet, Vladimir Smakhtin, Seong-mu Kang. The state of desalination and brine production: A global outlook. *Science of The Total Environment*. Volume 657,
2019, Pages 1343-1356, ISSN 0048-9697
21. El-Bourawi, M., Ding, Z. & Ma, R. e. a., 2006. A framework for better understanding mmebrane seperation process. *Journal of Membrane Science*, 285(1-2), pp. 4-29.
22. EMIS, 2010. *Membrane distillation*. [Online]
Available at: <http://emis.vito.be/techniekfiche/membrane-distillation?language=en>
[Accessed 04 03 2015].
23. Essalhi, M. & K., 2013. Self-sustained webs of polyvinylidene flouride electrospu nanofibres at different electrospinning times:1.Desalination by direct contact membrane distillation. *Journal of Membrane Science*, Volume 433, pp. 167-179.
24. Eugster, H., 1980. Geochemistry of evaporitic lacustrine desposits.. *Annual Review of Earth and Planetary Sciences*., Volume 8, pp. 35-63.
25. Field, R., Wu, H. & Wu, J., 2013. Multiscale Modelling of Membrane Distillation:Some Theoretical Considerations. *Industrial & Engineering Chemistry Research*, 52(26), pp. 8822-8828.
26. Gostoli, C. & Sarti, G., 1987. Low Temperature Distillation through Hydrophobic Membranes. *Seperation Science and Technology*, 22(2&3), pp. 855-872.
27. Gryta, M., 2001. Direct Contact Membrane Distillation with Crystallization Applied to NaCl Solutions.
28. Gunko, S., Verbych, S., Bryk, M. & Hilal, N., 2006. Concentration of apple juice using direct contatc membrane distillation. *Desalination*, Volume 190, pp. 117-124.
29. Hausmann, A., 2013. *Membrane Distillation in Dairy Processing*. s.l.:s.n.
30. Hausmann, A., 2013. *Membrane Distillation in Dairy Processing*, Melbourne: s.n.
31. Hsu, S., Cheng, K. & Chiou, J., 2002. Seawater desalination by direct contact membrane distillation. *Desalination*, Volume 143, pp. 279-287.
32. Imdakm, A. & Matsuura, T., 2005. Simulation of heat and mass transfer in direct contatc membrane distillation (MD):The effect of membrane physical properties.. *Journal of Membrane Science*, 262(1-2), pp. 117-128.
33. Khalifa, A. E. & Lawal, D. U., 2014. Flux Prediction in Direct Contact Membrane Distillation. *International Journal of Materials, Mechanics and Manufacturing*, 2(4), pp. 302-307.
34. Khayet, M. & Matsuura, T., 2001. Preparation and characterisation of Polyvinylidene Flouride Membranes for Membrane Distillation.. *Industrial and Engineering Chemistry Research*, 40(24), pp. 5710-5718.
35. Khayet, M., n.d. *Desalination by Membrane Distillation*. [Online]
Available at: <http://www.desware.net/DESWARE-SampleAllChapter.aspx>
[Accessed 03 03 2015].

36. König, A. & Weckesser, D., 2005. *Membrane Based Evaporation Crystallization*. s.l., s.n., pp. 1171-1176.
37. Kucera, J., 2010. *Reverse Osmosis: Industrial Applications and Processes*. Massachusetts(Salem): Scrivener Publishing LLC.
38. Kullab, A., 2011. *Desalination Using Membrane Distillation*, Stockholm: s.n.
39. Lagana, F., Barbieri, G. & Drioli, E., 2000. Direct contact membrane distillation: modelling and concentration experiments. *Journal of Membrane Science*, 166(1), pp. 1-11.
40. Liley, E. et al., 1999. Section 2: Physical and Chemical Data. In: D. W. Green, ed. *Perry's Chemical Engineers' Handbook*. 7th ed. s.l.:McGraw-Hill.
41. Mariah, L., 2006. *Membrane Distillation Of Concentrated Brines*, Durban: s.n.
42. Martinez, J. e. a., 2003. Estimation of vapour transfer coefficient of hydrophobic porous membranes for applications in membrane distillation.. *Seperation and Purification*, 33(1), pp. 45-55.
43. McCabe, W. L., Smith, J. & Harriott, P., 1993. Unit Operations of Chemical Engineering. Fifth Edition. In: B. J. Clark & E. Castelleno, eds. New York: McGraw-Hill Book Co, pp. 882-923.
44. Onsekizoglu, P., 2012. Membrane Distillation: Principle, Advances, Limitations and Future Prospects in. In: S. Zereshki, ed. *Distillation – Advances from Modeling to Applications*. s.l.:Intech, pp. 233-266.
45. Pantanja, C. e. a., 2016. Membrane Distillation Crystallisation Applied to Brine Desalination: Additional Design Criteria. *Industrial and Engineering Chemistry Research*, 55(4), pp. 1004-1012.
46. Payo, M. e. a., 1999. Air gap membrane distillation of aqueous alcohol solutions. *Journal of Membrane Science*, Volume 169, pp. 61-80.
47. Phattaranawik, J. & Jiratananon, A., 2003. Effect of pore size distribution and air flux on mass transport in direct contact membrane distillation. *Journal of Membrane Science*, 215(1-2), pp. 75-85.
48. Qtaishat, M. & Banat, F., 2012. Desalination by solar powered membrane distillation systems. *Desalination*, Volume 308, pp. 186-197.
49. Qtaishat, M., Matsuura, T., Kruczek, B. & Khayet, M., 2007. Heat and mass transfer analysis in direct contact membrane distillation. *Desalination*, 219(1-3), pp. 272-292.
50. Ramirez, C., Patel, M. & Blok, K., 2006. From fluid milk to milk powder: Energy use and energy efficiency in the European dairy industry. *Energy*, Volume 31, pp. 1984-2004.
51. Rao, G., Hiibel, S. & Childress, A., 2014. Simplified flux prediction in direct-contact membrane distillation using a membrane structural parameter. *Desalination*, Volume 351, pp. 151-162.
52. Salehi, M. & Rostamani, R., 2013. Review of membrane distillation for the production of fresh water from saline water. *Journal of Novel Applied Sciences*, Volume 2, pp. 1072-1075.
53. Salzman, W., 2004. *The Melting Curve for Water; Vapor Pressure*. [Online] Available at: <http://www.chem.arizona.edu/~salzmanr/480a/480ants/watvp/watvp.html> [Accessed 06 04 2016].
54. Shah, M. 2009. *Process Engineering: Agitation & Mixing*. Dharamsinh Desai University India, Short course material, www.dduanchor.org/site/.../Process-Engineering-Agitation-Mixing.pdf

55. Myers, K., Reeder, M., Fasano, J. 2002. *Optimizing a mixer by using the proper baffles*. CEP. <http://people.clarkson.edu/~wwilcox/Design/mixopt.pd>
56. Surapit, S., Jiratananon, R. & Fane, A., 2006. Mass transfer mechanisms and transport resistances in direct contact membrane distillation process.. *Journal of Membrane Science*, Volume 277, pp. 186-194.
57. Susanto, H., 2011. Towards practical implementations of membrane distillation. *Chemical Engineering and Processing:Process Intensification*, 50(2), pp. 139-150.
58. Tomaszewska, M., 2000. Membrane distillation-Examples of Applications in Technology and Environmental Protection.. *Polish Journal of Environmental Studies.*, 9(1), pp. 27-36.
59. Tun, C., Fane, A., Matheickal, J. & Sheikholeslami, R., 2005. Membrane distillation crystallization of concentrated salts—flux and crystal formation. *Journal of Membrane Science*, 07, 257(1-2), pp. 144-155.
60. University of Colorado at Boulder, 2015. *Organic Chemistry at CU Boulder*. [Online] Available at: <http://orgchem.colorado.edu/Technique/Procedures/Crystallization/Crystallization.html> [Accessed 21 04 2015].
61. Van Ness, H. C. & Abbott, M. M., 1999. Section 4: Thermodynamics. In: D. W. Green, ed. *Perry's Chemical Engineers' Handbook*. 7th ed. s.l.:McGraw-Hill.
62. Walton, J. e. a., 2000. *Seperation and Waste Heat Desalination by Membrane Distillation*, Texas: s.n.
63. World Bank Group, n.d. *Introduction to Wastewater Treatment Processes*. [Online] Available at: <http://water.worldbank.org/shw-resource-guide/infrastructure/menu-technical-options/wastewater-treatment> [Accessed 03 03 2015].
64. Wu, Y., Wang, R. & Field, R., 2014. Direct contact membrane distillation:An experimental and analytical investigatiuon of the effect of membrane thickness upon transmembrane flux.. *Journal of Membrane Science*, Volume 470, pp. 257-265.
65. Zeng, L. & Gao, C., 2010. The prospective application of membrane distillation in the metallurgical industry. *Membrane Technology*, 05, 2010(5), pp. 6-10.
66. Samant, K & O'Young, L. 2006. *Understanding crystallization and crystallizers*. Clear Water Bay technology inc.